Generation of high-resolution water surface slopes from multi-mission satellite altimetry

C. Schwatke[1], M. Halicki[2,1], and D. Scherer[1]

[1]Technical University of Munich, School of Engineering & Design, Department of Aerospace & Geodesy, Deutsches Geodätisches Forschungsinstitut (DGFI-TUM), Arcisstraße 21, 80333 München, Germany
[2]Department of Geoinformatics and Cartography, Faculty of Earth Sciences and Environmental Management, University of Wrocław, pl. Uniwersytecki 1, 50-137 Wrocław, Poland

Key Points:

- High-resolution water surface slopes (WSS) for 11 Polish rivers have been determined from almost 30 years of cross-calibrated multi-mission altimetry measurements.
- For the 8 rivers studied where *in-situ data* is available, we obtained a mean root mean square error of 26 mm/km, which decreases to 10 mm/km if 2 mountain rivers are excluded.
- For 6 rivers, the estimated WSS showed the highest accuracy compared to WSS datasets based on digital elevation models, ICESat-2, or lidar.

Corresponding author: Christian Schwatke, christian.schwatke@tum.de

Abstract

For nearly three decades, satellite radar altimetry has provided measurements of the water surface elevation (WSE) of rivers. These observations can be used to calculate the water surface slope (WSS), which is an essential parameter for estimating flow velocity and river discharge. In this study, we calculate a high-resolution WSS of 11 Polish rivers based on multi-mission altimetry observations from 11 satellites in the period from 1994 to 2022. The proposed approach is based on a weighted such gauge stations adjustment with an additional Laplace condition and an *a priori* gradient condition. The processing is divided into river sections not interrupted by dams and reservoirs. After proper determination of the WSE for each river kilometer (bin), the WSS between adjacent bins is calculated. To assess the accuracy of the estimated WSS, it is compared with slopes between gauge stations, which are referenced to a common vertical datum. Such gauge stations are available for 8 investigated rivers. The root mean squared error (RMSE) ranges from 3 mm/km to 80 mm/km, with an average of 26 mm/km. However, the mean RMSE decreases to 10 mm/km when the 2 mountain rivers are excluded. The WSS accuracies are also compared with those of slope datasets based on digital elevation models, ICESat-2 altimetry, and lidar. For 6 rivers the estimated WSS showed the highest accuracy. The improvement was particularly significant for mountain rivers. The proposed approach allows an accurate, high-resolution WSS even for small and medium-sized rivers and can be applied to almost any river worldwide.

Plain Language Summary

The Water Surface Slope (WSS) of a river is a measure of how steeply it flows downstream. This value affects the velocity of the water and also the force with which the water erodes the river bed. WSS is calculated by dividing the difference between two water surface elevations (WSE) by the length of the river section between these points. In this paper, we determine the WSS on almost every kilometer of 11 Polish rivers. For this purpose, we used almost 30 years of satellite altimetry measurements, which provide information about the height of the water surface at a given place and time. After filtering and mathematical adjustment of these measurements, we determined the WSE and WSS on almost every kilometer of the studied rivers. We compared our results with the average gradients between neighboring water level gauge stations, and for most rivers we obtained very small errors. Compared to other sources of WSS data, our method showed the highest accuracy. The results presented in this work are the first such accurate and spatially dense WSS information of Polish rivers. Moreover, the proposed method allows the determination of WSS on almost any river in the world.

1 Introduction

Water Surface Slope (WSS) is the difference in water surface elevation (WSE) between an upstream and downstream point on a river divided by the length of the reach (Ozga-Zielińska & Brzeziński, 1997). It is an important parameter in geomorphic and hydrologic modeling: the WSS determines the transport and erosion capacity of a river (Migoń, 2006), and is required to calculate the flow velocity (Manning, 1891) and the river discharge (e.g. Rantz, 1982; Bjerklie et al., 2003; Tarpanelli et al., 2013; Durand et al., 2014; Gleason & Durand, 2020). In general, a longitudinal river profile has the shape of a concave parabola, but the younger the river and the less uniform the structure of the river bed, the more this profile deviates from the parabolic shape (Dębski, 1970).

WSS can be calculated using several approaches. Continuous measurement of the WSE with a GNSS receiver mounted on a boat allows for an accurate WSS determination for the entire studied reach (e.g. Habel, 2010; Altenau et al., 2017; Pitcher et al., 2019). WSS can also be determined using airborne lidar, radar, or photogrammetry (e.g. Jiang et al., 2020a; Bandini et al., 2020). However, these methods are mostly used on

a local scale because of the high cost of a field campaign. The recently launched Surface Water and Ocean Topography (SWOT) satellite is expected to provide accurate WSS measurements even for rivers less than 100 m wide. So far, there have been several examples of the use of SWOT-like data from an airborne wide-swath altimeter (AirSWOT), which showed a promising ability to calculate WSS with a Root Mean Squared Error (RMSE) of 15 mm/km (Pitcher et al., 2019), 16 mm/km (Altenau et al., 2019) or 32 mm/km (Tuozzolo et al., 2019).

The WSS of a river can also be determined using a digital elevation model (DEM), such as the Shuttle Radar Topography Mission (SRTM) (LeFavour & Alsdorf, 2005; Paz & Collischonn, 2007) or the ALOS PALSAR RTC-DEM (Lamine et al., 2021). Cohen et al. (2018) developed a global river slope database using the HydroSHEDS DEM. Using the same DEM, Ruetenik (2022) developed a web application to generate longitudinal river profiles. However, since the vertical errors of global DEMs are considerable (e.g. the vertical error of the SRTM DEM is of several meters (Rodríguez et al., 2006)) and the spatial resolution of global DEMs is usually low, DEM-based WSS should only be calculated for long sections of large rivers (LeFavour & Alsdorf, 2005). Often DEMs such as the SRTM do not provide WSE for smaller rivers, but only the surrounding topography or averaged water levels for larger rivers. Furthermore, the inaccuracies of SRTM-based WSE significantly exceed the errors of WSE determination based on lidar data (Schumann et al., 2008). In addition, the data acquisition for a DEM is usually done in short time periods (e.g., a 10-day period in February 2000 for the SRTM DEM), but the WSS varies in time (Paris et al., 2016) so the observations may not represent the average WSS.

WSS can also be calculated from the WSE measured at neighboring gauges (Durand et al., 2014). The main advantage of this approach is its high accuracy and the possibility to observe the temporal variability of WSS. This approach also allows the calculation of an average WSS value for a given river section. However, the number of gauges has been decreasing over the last decades (Vorosmarty et al., 2001; Calmant & Seyler, 2006), and the spatial distribution of gauges is uneven (Hannah et al., 2011). In addition, some gauges are not referenced to a vertical datum, so the vertical difference between them cannot be calculated accurately. On poorly gauged rivers, the distance between neighboring gauges can be even hundreds of kilometers, making it impossible to capture the spatial variability of the river profile. Furthermore, this approach is not applicable to river sections with flow disturbances, such as waterfalls, dams, or weirs.

The gap in gauge measurements is partly filled by satellite altimetry, which has been providing WSE of oceans, wetlands, lakes, and rivers for more than 30 years (Abdalla et al., 2021). Currently operating altimetry missions can observe even small rivers (width < 100 m) with an RMSE of 20-30 cm (e.g. Halicki & Niedzielski, 2022; Jiang et al., 2020b; Kittel et al., 2021; Deidda et al., 2021). Using satellite altimetry, the WSE of rivers is observed at so-called virtual stations (VS), which are located at the intersection of the satellite ground track and the river channel. The quality of a VS's WSE time series can be improved by correcting it for the WSS bias that results from the orbit variation and thus a changing location of an altimeter measurement. This bias has been observed by Santos da Silva et al. (2010) and Boergens et al. (2016). Halicki et al. (2023) proposed two corrections based on gauge data and on Sentinel-3 altimetry observations and showed, that both corrections applied on 16 VS on the middle Oder River resulted in an average accuracy improvement of 25% (RMSE decrease from 22 cm to 16 cm). In some cases the RMSE reduction exceeded 50%. Also, Scherer et al. (2022a) corrected altimetry observations on rivers using ICESat-2 based WSS and obtained an improvement in RMSE up to 30 cm or 66%.

Since altimetry observations from a given mission are referenced to a common vertical datum, multiple VSs can be used to determine WSS (Birkett, 2002). However, WSE measurements at different VSs are observed at different times, so WSE variations can introduce errors in the derived WSS. Therefore, WSE averages at virtual stations (Tarpanelli

et al., 2013; Tourian et al., 2016; Halicki et al., 2023) or monthly means (O'Loughlin et al., 2013; Paris et al., 2016) are used. Satellite observations can also be used to model the longitudinal profile of the river. Using a least-squares approach based on multi-mission altimetry to derive a linear model of the Mississippi River yielded an average absolute median WSS error of 12 mm/km (Scherer et al., 2020). WSS can also be determined using laser altimetry (e.g. Hall et al., 2012; O'Loughlin et al., 2013). Using the unique measurement geometry of ICESat-2 with six parallel laser beams, Scherer et al. (2022a) derived reach-scale WSS both along and across the satellite ground track with a median absolute error of 23 mm/km.

Although the accuracy of satellite altimetry has improved significantly over the past decades, observations are still limited by low spatial coverage (e.g., equatorial track spacing of 311 km for the Jason satellites) and low temporal resolution (e.g., a revisit time of 27 days for the Sentinel-3 satellites). Since WSS can have strong temporal and spatial variability, altimeter observations from a single satellite may be too sparse to accurately determine the WSS variability along an entire river. However, by using observations from many different satellites (multi-mission approach), the temporal and spatial resolution of altimeter observations can be increased (e.g. Tourian et al., 2016; Bogning et al., 2018; Normandin et al., 2018).

In this paper, we present a new cross-calibrated multi-mission approach to determine the WSS of a river. Using altimeter observations from CryoSat-2, Envisat, ERS-1, ICESat-1/-2, Jason-2/-3, Sentinel-3A/-3B/-6A, and SARAL ranging from 1994 to 2022, we aim to obtain high-resolution WSS (every kilometer) of the largest Polish rivers within the accuracy requirement recommended for the SWOT mission (17 mm/km). We will assess the accuracy of this method using WSS derived from *in-situ* water levels, airborne lidar, ICESat-2, and DEMs.

This article is structured as follows: Section 2 describes the study area, which includes the 11 Polish river. In Section 3, the used altimeter data, SWORD data, and validation data are presented. In Section 4, the methodology for estimating WSS from satellite altimetry using a weighted least-squares adjustment is explained. The WSS results are then presented and a quality assessment is performed in Section 5. In Section 6, the WSS results of this study are discussed in the context of WSS from other sources. The paper concludes with a summary and an outlook.

2 Study Area

The study area includes 11 rivers in the Vistula and Oder basins, which are located in Central Europe and cover most of Poland (Fig. **??**). We selected only those rivers, whose centerlines are included in the "SWOT Mission River Database" (SWORD, see Section 3.2). The southern part of the study area is characterized by mountain ranges (Sudetes and Carpathians), whose heights do not exceed 2,500 m. North of them is an area of highlands, while in the central and northern part of Poland lowlands predominate. The river network in this area is characterized by a right-sided asymmetry: both the Vistula and the Oder rivers have many more tributaries from the east than from the west (Pociask-Karteczka, 2018). This asymmetry is closely related to the history of the development of the river network, which was shaped by numerous regressions and transgressions of the Scandinavian ice sheets and changes in the level of the Baltic Sea (Andrzejewski & Starkel, 2018).

The characteristics of the rivers studied are presented in Table 1. These rivers range in length from 174 km (Wisłoka) to 1,022 km (Vistula). The Vistula has the highest discharge (over 1,000 m^3/s). The discharge of the Oder is almost twice as low and amounts to 567 m^3/s. The area of the studied basins is more than 313,000 km^2, of which is about 62% and 38% for the Vistula and Oder basins respectively. Due to limited data avail-

ability (i.e. the SWORD dataset does not include upper river sections) and the presence of hydraulic structures, not all river sections are considered in this work. For large, lowland rivers, almost all sections are included (91%, 80%, and 72% for the Bug, Warta and Vistula rivers, respectively). Due to the large number of hydraulic structures, many sections of the Oder and Noteć rivers were excluded from this study. The average river width of the investigated sections, calculated on a basis of the SWORD database, ranges from 46 m (Noteć) to 299 m (Vistula). The narrowest sections are 42 m wide, while the widest sections were recorded on Bug (716 m) and Vistula (640 m). It should be noted, however, that fluvial lakes have been excluded from the river width calculations, as they may distort bias the river width values.

According to the world map of the Köppen-Geiger climate classification (Peel et al., 2007), the climate of the study area can be classified as humid continental, with an average annual precipitation of 610 mm (Miętus et al., 2022). The flow regime of Polish rivers has been proposed by Wrzesiński (2018), who followed the criteria of Dynowska (1997), using the relation of the average flow in spring or summer to the annual flow. In most of the studied reaches, the river regime is nival, with a high flow in the spring months. The mountain rivers in the south are characterized by the nival-pluvial regime, with high flows in the spring and summer months. The high spring flows are due to snowmelt, while the high summer flows are due to the intense precipitation.

Table 1. Characteristics of the rivers included in this study and of the river sections studied.

River	Recipient	Entire rivers*			Studied river sections**			
		Basin	Length	Discharge	Length	Width [m]***		
		[km^2]	[km]	[m^3/s]	[km]	Mean	Max	Min
Vistula	Baltic Sea	193,960	1,022	1,080	736	299	640	42
Oder	Baltic Sea	119,074	840	567	481	150	266	42
Warta	Oder	54,520	795	216	635	57	94	42
Bug	Narew	38,712	774	155	703	100	716	42
Narew	Vistula	74,527	499	313	232	123	430	42
San	Vistula	16,877	458	129	333	87	125	42
Pilica	Vistula	9,258	333	47	148	64	87	45
Wisłoka	Vistula	4,109	173	36	110	46	67	42
Dunajec	Vistula	6,796	249	86	161	72	92	45
Noteć	Warta	17,302	391	77	127	46	63	42
Poprad	Dunajec	2,081	174	26	108	49	63	42

* Source: (IMGW-PIB, 2013; Bielak et al., 2021)
** Calculations based on the SWORD data (Altenau et al., 2021a)
*** Fluvial lakes are excluded from this statistics.

3 Data

3.1 Altimeter Data

For about three decades, satellite altimetry has been successfully used to monitor WSE of rivers (Schwatke et al., 2015b; Villadsen et al., 2015; Tourian et al., 2017). In this study, WSE from multi-mission satellite altimetry are used as input data for the estimation of WSS along Polish rivers. For this purpose, the altimetry data are taken from the internal Multi-Version Altimetry (MVA) data holding of the Open Altimeter Database (OpenADB, https://openadb.dgfi.tum.de, (Schwatke et al., In Review)) developed by the Deutsches Geodätisches Forschungsinstitut der Technischen Universität München (DGFI-TUM). It provides altimeter measurements, altimeter waveforms, geophysical corrections,

and models needed to estimate WSE. Figure **??** shows the 11 altimeter missions divided into 18 orbit phases used in this study. The mission colors are chosen according to their orbit phase. The data used in this study were measured between the years 1994 and 2022.

The variety of satellite altimetry missions on different orbits contributes to a dense coverage of WSE observations along the rivers. In particular, missions with long repeat cycles or drifting orbits. These missions are ERS-1E (168 days), ERS-1F (168 days), CryoSat-2 (369 days), SARAL (DP, 35 days, drifting) and Jason-2 (GM, 16 days, drifting). Other missions with a short repeat cycle such as Jason-2/-3 (10 days), Sentinel-3A/-3B (27 days) or Envisat (35 days) without a drifting orbit, monitor the same river crossings with high temporal resolution but poor spatial resolution. ICESat-1 and ICESat-2 are a compromise between the two orbits mentioned above, with a lower repeat cycle of only 90 days, but a higher spatial resolution between the satellite tracks. Overall, the combination of the different types of altimeter missions is essential in this study to derive a high resolution WSS along the river.

3.2 SWORD Data

The "SWOT River Database" (SWORD) (Altenau et al., 2021b), developed for the "Surface Water and Ocean Topography" (SWOT) satellite mission, provides the spatial framework for this study. SWORD contains high-resolution river centerlines (30 m) and widths from the "Global River Widths from Landsat" (GRWL, Allen and Pavelsky (2018)) dataset. The centerlines are segmented into approximately 10 km long reaches and nodes with 200 m spacing. The reaches and nodes contain additional metadata, such as information on the location of artificial or natural river obstructions (i.e., dams and waterfalls). In addition, SWORD contains WSE and WSS data from MERIT Hydro (Yamazaki et al., 2019), a multi-error-removed improved-terrain DEM based on SRTM, which we use for comparison with the results of this study.

3.3 Validation Data

3.3.1 Gauge-based WSS

To validate the WSS obtained in this study, we use WSE data from 81 gauges of the Institute of Meteorology and Water Management – National Research Institute (Instytut Meteorologii i Gospodarki Wodnej – Państwowy Instytut Badawczy, IMGW-PIB). For this study, we use hourly WSE measurements from January 2016 to May 2022 from the publicly available IMGW-PIB database (`https://danepubliczne.imgw.pl/datastore`, accessed on 2022-09-01). This dataset consists of 4,479,052 measurements, representing 98.38% of the available data for this period. Therefore, no gap interpolation was performed. In addition to the WSE data, we used gauge-zero values referenced to the Kronsztadt'86 vertical datum (IMGW-PIB, 2013). Because of the common vertical datum of all 81 gauges, it was possible to calculate the WSS between adjacent stations without hydraulic structures in between.

3.3.2 Lidar-based WSS

We use airborne laser scanning (ALS) lidar data to extract an *in situ* river profile for validation. The lidar data are provided by the Polish Head Office of Geodesy and Cartography (Główny Urząd Geodezji i Kartografii) via `geoportal.gov.pl` (Kurczyński, 2015). The ALS campaigns started in 2010 with reference to the height system "PL-KRON86-NH". From 2018 to 2021 (the latest available data), the lidar point clouds are referenced to the European vertical reference frame "PL-EVRF2007-NH" height system. The study areas are not completely covered by a single ALS campaign, and the lidar data were acquired on different dates within one year. Since the water level of the studied rivers varies significantly, the WSS can only be calculated in reaches with lidar data from the same

date and not all reaches are covered. For each point along the SWORD river centerline, class 9 (water) records are extracted from the lidar point cloud within 15 m of the centerline. This was selected in order to avoid using lidar measurements contaminated by the river shore. If more than 500 records can be extracted, the median elevation is assigned to the centerline point. Additionally, the standard deviation of the elevations of the extracted points is used for outlier detection. However, the results can still be affected by land contamination. Furthermore, temporal WSS variations can affect the lidar WSS so that it does not represent the mean WSS.

3.3.3 ICESat-2 River Surface Slope

The reach-scale "ICESat-2 River Surface Slope" (IRIS, Scherer et al. (2022b, In Review)) dataset is used to evaluate the results of this study. IRIS is derived for each SWORD reach (Altenau et al., 2021a) from observations of the spaceborne lidar sensor ATLAS onboard ICESat-2. Since ICESat-2 measures synchronously along six beams, the WSS can be calculated across all beams intersecting the respective reach (Scherer et al., 2022a). In addition, due to the high accuracy and precision of the ICESat-2 observations, the WSS is also calculated along a single beam if it intersects the river nearly parallel. In this study, we use the combination of the across- and along-track methods for comparison. Compared to the results of this study, the spatial resolution of IRIS is lower as it corresponds to the SWORD reach length of about 10 km. However, IRIS data are homogeneously distributed along the river and are therefore available where *in situ* data may be missing. IRIS has been validated against 815 reaches in Europe and North America with a median absolute error of 23 mm/km (Scherer et al., 2022a).

3.3.4 DEM-based WSS

To assess the accuracy of our results, we also use WSS datasets based on DEM models. The WSS from the SWORD database have already been described in Section 3.2. Furthermore, we use the "Global River Slopes" (GloRS) database, developed by Cohen et al. (2018). Here, the authors calculated the WSS based on the 15 arc-sec resolution (∼460x460 m) "SHuttle Elevation Derivatives at multiple Scales" (HydroSHEDS) DEM and stream-network (Lehner et al., 2008). The proposed approach consisted of calculating the maximum and minimum elevations of each river segment and dividing the elevation difference by the length of the segment. For a global analysis, the authors upscaled the 15 arc-sec DEM to a 6 arc-sec model (1 arc-sec ∼ 30 m at the equator).

Another DEM-based analysis of river profiles was recently presented by Ruetenik (2022), who developed the "RiverProfileApp" (`https://riverprofileapp.github.io`, accessed on 2023-01-25). This tool allows an almost global analysis of river profiles with a resolution of 90 m. The "RiverProfileApp" offers two DEM models. To extract river profiles, we use the default HydroSHEDS flow direction grid for flow routing. In addition, a smoothing window size of 10 km is applied to the calculated profiles. To obtain WSS based on the river location and elevation, we perform the following calculations: (1) for each river coordinate, the nearest SWORD centerline and chainage is assigned, (2) due to the amount of data noise, we average the elevations for each river kilometer using a 30 km window (15 km upstream and 15 km downstream), (3) elevations with a dam or river lake within the window are discarded, (4) for each river kilometer, the WSS is calculated by comparing its elevation to the neighboring river kilometer elevation. These values (30 km window and 1 km distance) were obtained by minimizing the noise of slope variations and comparing the obtained slopes with *in situ* data.

4 Methodology

In this section, the new innovative approach for the generation of high-resolution water surface slopes from cross-calibrated multi-mission satellite altimetry is described in detail.

The approach consists of six processing steps which are shown in the flowchart in Figure **??** and described in the following sections. The method is explained using an example section of the Vistula River between chainage 0 km and 211 km.

4.1 SWORD River Centerline

For each river, a high-resolution centerline is derived from the SWORD (Altenau et al., 2021a) dataset described in Section 3.2. It provides reaches (∼10 km), nodes (∼200 m) and centerlines (∼30 m) for rivers worldwide. In this approach, we estimate the mean slope of the water surface with a spatial resolution of 1 km along the river centerline. For this purpose, the high-resolution centerlines are grouped into 1 km bins, which serve as reference points in this approach. In addition, each centerline point is mapped to its reference point, so that each altimeter crossing can be mapped exactly to the corresponding reference point, but also the centerline point on the river. Figure **??** shows an example section of the Vistula River between chainage 52 km and 88 km with the extracted SWORD centerline highlighted in black and the reference points as black dots along the centerline.

4.2 Area of Interest (AOI)

To extract the relevant altimeter data across the river, we use the SWORD centerline from the last step as input. Since there are valid altimeter measurements not only over the river, but also several hundred meters close to the river due to the size of the altimeter footprint (Boergens et al., 2016; Schwatke et al., 2015a), we create an AOI with a boundary of 1000 m from the SWORD centerline. This allows us to extract altimeter data that measures the river and not land or adjacent waters. The AOI derived from the SWORD centerline is shown in Figure **??**. It is highlighted in white in the background.

4.3 Water Levels at River Crossings using Satellite Altimetry

Using the AOI of the river of interest, we extract the high-frequency altimeter measurements of the 11 altimeter missions introduced in Section 3.1 from OpenADB (Schwatke et al., In Review). The combination of measurements from altimeter missions on different orbits increases the number of river crossings and thus the spatial resolution along the river.

Since the altimeter missions have different orbits, the crossing of the river of interest is random, which also depends on the river topology. Rivers that flow in an east-west direction have a higher probability of being crossed than rivers that flow in a north-south direction, because the altimeter tracks also run in a north-south direction. Figure **??** shows the distribution of crossing altimeter tracks within the AOI for the example section of the Vistula River. It clearly shows the missions with a short repeat cycle between 10 days and 35 days such as Envisat, Jason-2/-3, Jason-2/-3 (EM), Sentinel-3A/-3B, SARAL, and Sentinel-6A, where many altimeter tracks cross the river side by side. More important for our approach are altimeter missions that fill in the data gaps along the river. Therefore, altimeter missions with long repeat cycle (CryoSat-2, ICESat-1/-2) or a drifting orbit (ERS-1E/-1F, SARAL (DP), Jason-2 (GM)) are more suitable. By combining both types of altimeter missions, a good data coverage along the river can be achieved, as shown in Figure **??**.

Table 2 gives an overview of the used river crossings per mission and river. The number of valid river crossings depends on the length of the river, but also on the width of the river. A comparison between the Dunajec (161 km studied river length) and the Oder (481 km studied river length), which is 3 times longer, shows that about 15 times more valid river crossings are available for the Oder (6,808) than for the Dunajec (451). This is mainly due to the data quality for small river crossings, but the river course can also have an influence.

Table 2. Number of used river crossings by mission and river

Mission	Vistula	Oder	Warta	Bug	Narew	San	Pilica	Wisłoka	Dunajec	Noteć	Poprad
Cryosat-2 (LRM)	751	785	696	652	307	230	208	53	80	188	8
Envisat	566	368	600	393	186	156	151	80	17	68	3
Envisat (EM)	101	75	96	98	47	11	9	9	2	33	-
ERS-1E	25	14	26	24	7	10	8	2	-	11	-
ERS-1F	32	24	24	24	12	10	9	-	4	7	-
ICESat-1	33	39	40	27	10	3	11	-	8	14	-
ICESat-2 (GT1L)	250	192	159	136	51	50	46	7	29	55	10
ICESat-2 (GT1R)	255	200	165	144	55	57	46	8	29	57	14
ICESat-2 (GT2L)	144	204	156	141	73	61	45	7	21	64	12
ICESat-2 (GT2R)	264	201	172	167	72	66	44	9	27	82	11
ICESat-2 (GT3L)	249	185	172	146	68	59	47	12	29	65	11
ICESat-2 (GT3R)	249	206	174	154	58	57	50	10	31	70	9
Jason-2	895	606	519	522	299	170	209	-	4	240	69
Jason-2 (EM)	50	61	52	76	19	1	10	29	20	20	-
Jason-2 (GM1)	88	73	89	81	26	28	23	12	6	31	4
Jason-2 (GM2)	86	72	88	74	25	26	24	9	9	32	1
Jason-3	869	617	442	366	222	130	183	-	-	179	33
Jason-3 (EM)	50	69	58	82	22	-	4	24	1	22	-
SARAL	267	255	354	280	126	93	87	32	24	93	5
SARAL (DP)	419	491	532	448	200	141	164	29	38	183	13
Sentinel-3A	561	506	541	402	225	227	96	83	-	199	13
Sentinel-3B	319	314	284	284	106	109	68	5	72	104	-
Sentinel-6A (LR)	285	196	171	121	62	38	54	-	-	55	36
All Crossings	6,808	5,753	5,610	4,842	2,278	1,733	1,596	420	451	1,872	252

To estimate the water levels at the river crossings, the necessary altimeter measurements, geophysical corrections and models are extracted from OpenADB. When processing the water levels, an individual analysis of the radar echoes, called retracking, is applied. Therefore, the Improved Threshold Retracker (Hwang et al., 2006) is used, which is optimized for inland waters. The combination of water levels from different altimeter missions requires the consideration of range biases caused by systematic effects, which are computed by a multi-mission crossover analysis (Bosch et al., 2014).

$$\begin{aligned} \mathtt{WSE} \;=\; & \mathtt{H}_{\mathtt{sat}} - \mathtt{R}_{\mathtt{ralt}} - \mathtt{N} - \Delta\mathtt{h}_{\mathtt{ionos}} - \Delta\mathtt{h}_{\mathtt{wtrop}} - \\ & \Delta\mathtt{h}_{\mathtt{dtrop}} - \Delta\mathtt{h}_{\mathtt{etide}} - \Delta\mathtt{h}_{\mathtt{ptide}} - \Delta\mathtt{h}_{\mathtt{rbias}} \end{aligned} \tag{1}$$

Equation 1 shows the formula and parameters used to estimate the water levels of each altimeter measurement along the crossing altimeter tracks. The WSE is computed by subtracting the retracked altimeter range ($\mathtt{R_{ralt}}$), geoid height ($\mathtt{N}$), geophysical corrections and range bias ($\Delta\mathtt{h_{rbias}}$) from the satellite height $\mathtt{H_{sat}}$ to obtain the physical heights used in the next processing steps. The altimeter range is corrected by the geophysical corrections such as ionosphere ($\Delta\mathtt{h_{ionos}}$), wet troposphere ($\Delta\mathtt{h_{wtrop}}$), dry troposphere ($\Delta\mathtt{h_{dtrop}}$), Earth tides ($\Delta\mathtt{h_{etide}}$), and Pole tides ($\Delta\mathtt{h_{ptide}}$).

However, an outlier rejection is necessary before using the water levels in our new approach. There are several reasons for outliers, such as off-nadir measurements (Boergens et al., 2016), adjacent waters, or waveforms distorted by land contamination. Therefore, we apply an iterative outlier rejection on each crossing altimeter track in order to use only the most accurate altimeter measurements. To do this, we estimate the median water level for the altimeter track and the standard deviation of the differences. Then, water levels are rejected as long as the standard deviation is greater than 10 cm or the number of along-track altimeter measurements is greater than 5. Using a minimum of 5 altimeter measurements ensures that the later water level of the river crossing is based on multiple altimeter measurements and is therefore more accurate. After the outlier rejection, the median water level and the corresponding standard deviation of the water levels are assigned to the river crossing and used as input data in the next processing steps.

4.4 Water Levels for each River Section with Least-Squares Adjustment

In this section, the approach for estimating the water levels along the river with a spatial resolution of 1 km is described. We demonstrate this approach, which is based on a weighted least-squares adjustment, in detail on a river section of the Vistula River between chainage 0 km and 211 km. However, there may still be erroneous water levels in the data at this point because the consistency of neighboring water levels has not yet been considered in the along-track outlier rejection step above. For this purpose, we apply a Support Vector Regression (SVR, Smola and Schölkopf (2004)) to the water levels of each river section to rejected clear outliers of several meters. Figure **??** shows the valid water levels at the Vistula River section color-coded by altimeter mission. One can clearly see the influence of the different altimeter missions on the data distribution along the river. For example Jason-2/-3 and Sentinel-6A cross the river only near the 12 km river chainage. However, ICESat-1/-2 and CryoSat-2 are more evenly distributed along the river than the other missions. As mentioned before, a combination of water levels from different altimeter missions is essential for an accurate estimation of WSE and WSS, respectively.

In the next step, we describe the applied weighted least-squares adjustment to estimate the water level for each 1 km bin. In the example of the Vistula River reach between 0 km and 211 km, water levels are calculated for 211 nodes n every kilometer. In addition, 1,578 water levels from altimeter measurements m at the river crossing are used as input data.

In the general least-squares adjustment formula, only observations $\mathbf{l}$ in the design matrix $\mathbf{A}$ without weighting are used to estimate the unknown water levels at each node $\mathbf{x}$ (Niemeier, 2008). Equation 2 shows the modified weighted least-squares adjustment formula compared to the general least-squares adjustment described in Niemeier (2008) which is used to estimate the water levels at each reach river node.

$$\underset{n\times 1}{\mathbf{x}} = (\underset{n\times k}{\mathbf{A^T}} \cdot \underset{k\times k}{\mathbf{P}} \cdot \underset{k\times n}{\mathbf{A}})^{-1} \underset{n\times k}{\mathbf{A^T}} \cdot \underset{k\times k}{\mathbf{P}} \cdot \underset{k\times 1}{\mathbf{l}} \tag{2}$$

In this study, however, we extended the design matrix **A** by two additional conditions, so that the design matrix **A** finally consists of three sections, which are introduced as follows.

- *Altimeter measurements*: In the first section of the design matrix **A**, the water levels of the altimeter measurements are assigned to the corresponding node. In the design matrix **A**, the corresponding node is set to 1 and the value of the water level is added to the observation vector **l**.
- *Laplace condition*: Since water levels are not available for all nodes, an additional Laplace condition was added to the design matrix **A** to ensure that it is not singular and still solvable. This Laplace condition can be thought of as an interpolation and smoothing filter that minimizes the differences between the water level of the current node and the previous and next nodes. In the design matrix **A** a filter of `[1 -2 1]` is applied to each node, except for the first and last node. The value in the observation vector **l** is set to 0. However, this may result in constant water levels at the boundaries of the river sections if no data is available.
- *A priori gradient condition*: To get rid of the problem at the boundaries caused by the Laplace condition, an additional *a priori* gradient condition has been added to the design matrix **A**. In the design matrix **A**, a filter of `[-1 1]` is applied to each node and the *a priori* water surface gradient is added to the observation vector **l**. The *a priori* water surface gradient is calculated by estimating a linear trend within a 20 km moving window along the river. This condition ensures that the resulting water levels at the boundaries do not converge to constant water levels, but take into account the *a priori* water surface gradient.

The dimension of the design matrix **A** consists of k rows and n columns where $k = 2n+m-2$, m is the number of altimeter measurements, $n-2$ is the number of rows of the Laplace condition and n is the number of rows of the *a priori* gradient condition.

Additionally, also a weighting of the three sections is applied in the matrix **P**. This is necessary to control the impact of the altimeter measurements, the *a priori* gradient condition, but also the smoothing of the Laplace condition along the river. The weights of the three groups were chosen empirically by validating the resulting water surface slopes with *in situ* data and with lidar data. This resulted in the following weights for the altimeter measurements (0.1), the Laplace condition (10.0), and the *a priori* gradient condition (5.0), which are set to the diagonal values of the identity matrix **P**.

The advantage of the weighted least-squares adjustment is that the associated water level errors for each node can be estimated by computing the covariance matrix $\mathbf{K_{xx}}$ using the formula described in Niemeier (2008).

Figure **??**, shows the resulting water levels (black line) of the introduced least-squares approach for the river section along the river. It can be clearly seen that the estimated water levels describe the average water level of the river very well. The seasonal water level variations and the uneven distribution of water levels are also well captured.

4.5 Water Surface Slopes for each River Section

In the final step, the water levels along the river are converted to WSS. Between two neighboring river nodes, the difference in WSE is calculated and divided by the length of the river from the SWORD centerline between them. The WSS errors are calculated in the same way. Figure **??** shows the resulting WSS and errors for the example section of the Vistula River.

5 Results and Quality Assessment

The new, innovative approach for generating high-resolution water surface slopes from multi-mission satellite altimetry is based on global, freely available data: river centerlines from SWORD and altimetry measurements from OpenADB. Therefore, this approach can be applied globally to almost any river. In this study, we present the WSS analysis of 11 Polish rivers, including sections located in lowland, upland, and mountainous areas (Section 5.1). Due to the dense network of gauges, referenced to a common vertical datum, we are able to assess the WSS accuracy by comparing it with the river slopes between adjacent gauges (Section 5.2). Furthermore, we perform a quality assessment based on cross validation (Section 5.3). Finally, to prove the usefulness of the WSS, we apply the river altimetry slope bias correction (Halicki et al., 2023) to the Sentinel-3B water level time series over two virtual stations (VS – intersections of satellite ground tracks and river channels) located in mountainous areas (Section 5.4).

5.1 WSS of Polish Rivers

Figure **??** shows the WSS of 11 Polish rivers. These results are also provided as NetCDF and shapefile, freely available at `www.zenodo.org/10.5281/zenodo.7709474` (Schwatke et al., 2023b). For most of the rivers, the WSS ranges from 0 to 500 mm/km. The steepest rivers occur in the southern, mountainous area – the WSS of Dunajec, Poprad and San (in their upper part) ranges from 1,000 mm/km to 4,000 mm/km. In general, the WSS of each river decreases in the downstream direction. On the contrary, the slope of the Noteć River slightly increases towards its mouth, but it is a highly regulated, lowland river with low WSS values on the whole studied section. It is also worth mentioning, that the WSS of most of the rivers is strongly variable in the spatial domain. For example, the WSS of the Vistula River changes by up to 200 mm/km every few kilometers. The most stable WSS can be found on the Pilica River, for which the slope values vary in the range of 350 mm/km to 500 mm/km almost along the whole studied section.

WSS variations can also be clearly seen in Figure **??**, which shows the Vistula (a), Oder (b), Warta (c), and Dunajec (d) rivers. Vistula, Oder, and Warta are the longest rivers in Poland. On the other hand, Dunajec is mainly located in a mountainous area with the highest WSS. The graphs showing the WSS variation of the other investigated rivers are presented in the appendix (Figures **??** and **??**). The WSS of the Oder and Warta rivers (Figure **??**b, c) varies by about 50-100 mm/km. The WSS variations on the Vistula (Figure **??**a) are even stronger with up to 250 mm/km. These variations are less significant on the Dunajec (Figure **??**d), compared to its total WSS of up to 4,000 mm/km.

The graphs in Figure **??** also include WSS errors (gray, vertical bars), which are related to the vertical errors of WSE in each of the 1 km bins (see Section 4.4). In general, large errors appear at the edges of the sections due to the lower number of WSE measurements. In addition, Figure **??** includes (1) the minimum, maximum and median WSS between neighboring gauges, (2) WSS from the SWORD database, (3) ICESat-2 based WSS from the IRIS database, and (4) WSS calculated from lidar data (see Section 3.3.2). A comparison between the different WSS will be made in the following sections.

5.2 Validation with In Situ Slopes

In order to assess the accuracy of the derived WSS of Polish rivers, we compare it with the *in situ* WSS between gauging stations. This comparison is not possible for Wisłoka, Noteć, and Poprad, due to the lack of connected gauges undisturbed by hydraulic structures. The median, maximum, and minimum *in situ* slopes of the Vistula, Oder, Warta, and Dunajec are shown in Figure **??**. The *in situ* slopes are more variable over short river sections since the vertical difference between the gauges is divided by a smaller length.

To properly compare the high-resolution, altimetry based WSS with *in situ* slopes, we calculate the mean WSS for each river section between selected gauges. These values for sections between neighboring gauges are presented in Figure **??** with black, horizontal lines. At the Vistula River, the lower and middle sections agree better than the upper section, but the differences do not exceed 50 mm/km. The derived WSS variation is generally within the *in situ* slope variation, especially for short gauge sections. The WSS of the Oder and Warta are almost identical to the *in situ* slopes, with very small differences. Also for the Dunajec River the agreement is very high for most of the sections, except for the most upstream section, where the difference exceeds 200 mm/km.

The accuracy of the estimated WSS from satellite altimetry of Polish rivers is presented in Table 3 (In-Situ RMSE). The RMSE value for each river (except for Wisłoka, Noteć, and Poprad) is given for each river section between flow disturbances, as well as for the entire river. The values in brackets refer to the number of gauged sections included in the RMSE calculation. The RMSE for the whole rivers ranges from 3 mm/km to 80 mm/km, with an average of 26 mm/km. The RMSE of more than half of the rivers studied (5 out of 8) is less than 15 mm/km. The lowest RMSE is 3 mm/km (Pilica), but this value is based on only three gauged river sections. However, the Bug and Oder rivers have comparatively small errors (4 mm/km and 6 mm/km, respectively), which were are based on 67 and 45 gauging sections, respectively. The derived WSS of the largest Polish river (Vistula) also shows a very good agreement with the *in situ* WSS (RMSE: 12 mm/km). However, the accuracy is significantly higher in the lower and middle sections (10 mm/km and a0 mm/km RMSE for the 0-211 km and 255-647 km sections, respectively) than in the upper section (28 mm/km RMSE). The only two rivers with RMSE above 30 mm/km are Dunajec (69 mm/km) and San (80 mm/km), which are located in a mountainous and upland areas and their slopes can locally reach between 2,000 mm/km and 4,000 mm/km.

5.3 Internal Cross-Validation of WSS

Using the method described in section 5.2, we can only compare the average WSS between two gauges. In this section, we perform an internal cross-validation of the derived WSE and WSS to evaluate the quality of the river sections not covered by gauges. It is also used to estimate the accuracy of the variability of the WSS along the river.

For the cross-validation, we calculate a WSS between each possible combination of two altimeter heights from Section 4.3 and compare them with our mean WSS between the two river crossings. Due to the large number of combinations (e.g. Warta: $>$ 300,000) and the different track lengths, this allows a robust internal validation of the WSS. Based on the WSS differences of all pairwise comparisons, the root mean square deviation (RMSD) is calculated for each river section and for the entire river.

Table 3 shows the results of the cross-validation (Cross-Val. RMSD) for each studied river section and for the whole river. For the Vistula, Oder, Warta, Bug, Narew, San, and Pilica rivers, the RMSE of the cross-validation varies between 16 mm/km and 32 mm/km. However, for the rivers Wisłoka, Dunajec, Noteć, and Poprad, the RMSD of the cross-validation is significantly larger and varies between 89 mm/km and 300 mm/km. This is mainly influenced by the smaller river width and the mountainous regions where three of the rivers are located. Table 3 clearly shows that the RMSD increases in the upstream direction.

5.4 Correcting Water Level Time Series from Satellite Altimetry for the Ground Track Shift Bias

Orbit perturbations cause a shift of the satellite ground tracks, which, for example, for Sentinel-3 can vary up to $\pm$1 km. Therefore, the locations of radar altimetry measurements for a single VS are not stationary. Since rivers are inclined water bodies, the

Table 3. Quality assessment and validation of estimated water surface slopes from satellite altimetry

River	Section [km]	In-Situ RMSE [mm/km]		WSS Mean ± STD [mm/km]	Cross-Val. RMSD [mm/km]	
Vistula	all	12	(82[1])	227 ± 72	16	(151,467[2])
	0 - 211	10	(10)	172 ± 47	23	(15,855)
	255 - 647	10	(66)	245 ± 72	15	(67,623)
	648 - 779	28	(6)	263 ± 58	14	(67,989)
Oder	all	6	(45)	225 ± 105	27	(161,860)
	2 - 442	6	(45)	216 ± 96	13	(79,464)
	639 - 680		n.a.	321 ± 143	35	(82,396)
Warta	all	25	(67)	265 ± 140	32	(303,700)
	0 - 485	25	(66)	201 ± 73	12	(100,561)
	502 - 562	5	(1)	442 ± 92	28	(101,239)
	562 - 647		n.a.	501 ± 82	47	(101,900)
Bug	all	4	(45)	183 ± 73	17	(322,276)
	0 - 647	4	(45)	177 ± 69	13	(160,748)
	659 - 715		n.a.	255 ± 81	20	(161,528)
Narew	all	12	(6)	102 ± 58	27	(17,570)
	0-21		n.a.	88 ± 33	58	(56)
	39-250	12	(6)	103 ± 60	27	(17,514)
San	all	80	(11)	579 ± 395	32	(24,911)
	0 - 30		n.a.	325 ± 23	27	(198)
	30 - 176	84	(10)	306 ± 99	20	(7,212)
	176 - 300	10	(1)	743 ± 309	35	(8,740)
	300 - 334		n.a.	1,376 ± 167	37	(8,761)
Pilica	all	3	(3)	436 ± 36	23	(13,794)
	0 - 131	3	(3)	437 ± 36	15	(6,879)
	154-171		n.a.	426 ± 34	29	(6,915)
Wisłoka	all		n.a.	556 ± 208	92	(3,136)
	0 - 57		n.a.	452 ± 107	37	(891)
	57 - 73		n.a.	426 ± 61	63	(1,024)
	73 - 110		n.a.	771 ± 196	131	(1,221)
Dunajec	all	69	(9)	1,994 ± 1,235	206	(4,295)
	0 - 70	35	(3)	791 ± 333	54	(1,092)
	96 - 173	80	(6)	2,772 ± 847	236	(1,595)
	184 - 200		n.a.	3,507 ± 260	236	(1,608)
Noteć	all		n.a.	107 ± 62	89	(4,348)
	0 - 49		n.a.	157 ± 32	30	(759)
	54 - 64		n.a.	125 ± 28	69	(796)
	113 - 156		n.a.	58 ± 48	106	(937)
	156 - 171		n.a.	40 ± 14	105	(927)
	171 - 181		n.a.	154 ± 26	98	(929)
Poprad	all		n.a.	2,505 ± 878	300	(542)
	0 - 64		n.a.	2,599 ± 1,058	69	(54)
	64 - 91		n.a.	2,030 ± 278	335	(223)
	99 - 116		n.a.	2,906 ± 95	297	(265)

[1] *Number of In-Situ Section,* [2] *Number of Water Levels from Satellite Altimetry*

Table 4. Validation of WSS from satellite altimetry with in-situ WSS. Additional quality assessment between WSS from DEM, SWORD, ICESat-2, and lidar with in-situ WSS

River	Gauge sections	RMSE [mm/km]					
		This study	Ruetenik (2022)	Cohen et al. (2018)	Altenau et al. (2021a)	Scherer et al. (2022b)	Lidar
Vistula	82	12	35	442	68	16	17
Oder	45	6	27	363	40	33	16
Warta	67	25	32	634	64	32	38
Bug	45	4	20	452	29	6	42
Narew	6	12	26	508	30	9	22
San	11	80	51	294	97	87	185
Pilica	3	3	68	496	68	5	183
Dunajec	9	69	232	2,742	273	386	168
Mean	-	26	65	732	86	81	84

altimeter measurements are subject to a bias that depends on the local WSS the distance between the actual measurement and the VS reference position. The WSS described in this study is estimated for each river kilometer, therefore it is possible to correct the WSE time series for the bias using the WSS for the river section exactly at the VS location.

Determining the exact location of an altimetry measurement can be challenging when a river section is parallel to the satellite ground track. Since the footprint size of radar altimetry measurements is generally greater than one kilometer, some WSE may be biased by off-nadir measurements. In these cases, the exact location of the satellite measurement cannot be accurately determined, and thus the WSE time series cannot be properly corrected for the WSS. Since the aim of this analysis is to prove the usefulness of the estimated WSS, we select two VS of the Sentinel-3B satellite from DAHITI, located on mountainous stretches of the San (DAHITI-ID: 41491) and Dunajec (DAHITI-ID: 41492) rivers, where the problem described above does not occur. We correct these VS for the WSS bias using the results of this study, which are 553 mm/km and 1,045 mm/km for the San and Dunajec VS, respectively.

To assess the improvement of the correction, we compare the uncorrected and corrected WSE time series of each VS with measurements from adjacent IMGW-PIB gauges, which are located 3.1 km and 3.3 km downstream of the San and Dunajec VS, respectively. All three time series (*in situ*, uncorrected and corrected) are shown in the upper graph in Figure **??** and Figure **??** for the San and Dunajec VS, respectively. The distance between the altimetry measurement and the VS reference position is presented in the middle plot (blue bars). The lower plot shows the error bars of the uncorrected (red bars) and corrected (green bars) measurements. The bias correction results in a significant reduction of the RMSE: from 0.36 m to 0.21 m (42%) for the San VS (DAHITI ID: 41491) and from 0.49 m to 0.29 m (41%) for the Dunajec VS (41492). Errors are reduced for most of the measurements. However, VS in mountainous areas are affected by larger errors than VS in lowland river sections, mostly due to the surrounding topography (Jiang et al., 2020b). Therefore, the WSE time series may still contain outliers, even though an outlier rejection has been performed in the DAHITI approach. In these cases, the bias correction does not reduce the measurement error.

6 Discussion

Table 4 shows the accuracy of WSS results from this study with WSS derived between gauging stations. In addition, the accuracy of other WSS datasets, based on DEM models (GLoRS (Cohen et al., 2018), RiverProfileApp (Ruetenik, 2022) and SWORD (Altenau et al., 2021a)), lidar (Section 3.3.2), and ICESat-2 from the IRIS dataset (Scherer et al., 2022b) with WSS derived between gauging stations is shown. Table 4 includes only 8 of the 11 studied rivers, because on Noteć, Wisłoka, and Poprad there are no gauge sections undisturbed by hydraulic structures. In general, the mean RMSE of the WSS derived in this study is significantly lower compared to the other approaches. The only two exceptions are the Narew River, where the accuracy of the ICESat-2 WSS (9 mm/km RMSE) slightly exceeds the accuracy of this study (12 mm/km RMSE), and the San River, where the accuracy of the WSS based on the RiverProfileApp (51 mm/km RMSE) exceeds the accuracy of this study (80 mm/km RMSE).

The GLoRS dataset is the least accurate with a mean RMSE of 732 mm/km. The accuracy of the SWORD WSS is also poor, with a mean RMSE of 86 mm/km and a minimum RMSE of 29 mm/km. The RiverProfileApp is the best DEM-based approach with an average RMSE of 65 mm/km. Although the RiverProfileApp is also based on a global DEM model, the processing uses a different approach than the GLoRS and SWORD databases (see Ruetenik (2022)). The RiverProfileApp allows the parameters to be set manually via the web application. However, this application does not provide WSS directly but generates river profiles downstream of a selected point. Based on this data, we calculate the WSE for each kilometer by averaging heights within a 30 km moving window (15 km upstream and 15 km downstream). Next, we calculate the WSS by comparing adjacent WSE. However, even though the RiverProfileApp revealed the highest accuracy among the DEM-based slopes, it was still significantly less accurate than WSS from multi-mission satellite altimetry approach. The low accuracy is probably caused by the coarse resolution of global DEM models, which in the area of small and medium-sized river channels causes large vertical errors. Furthermore, the mean RMSE values are strongly deteriorated by the high RMSE on the Dunajec River.

The RMSE of the WSS from airborne lidar is low for most of the lowland rivers. On the contrary, the RMSE for the mountain rivers is significantly higher (168 mm/km and 185 mm/km for the Dunajec and San rivers, respectively). The RMSE of the lidar-based WSS for the Pilica River is also high with 183 mm/km. The WSS from lidar is not well suited for validation because it does not represent a mean WSS but only a short temporal sample and lidar can be distorted over water. However, it has a high spatial resolution. Therefore, it can be used to interpret the quality of the spatial variations of our results, which are not visible in the WSS from gauges. The overall frequency of the spatial variations is in good agreement between our results and the lidar WSS, although the local extremes are not always in perfect agreement, possibly due to temporal variations. Specific features, such as the significantly increasing WSS between chainage 100 km and 125 km at the Dunajec River or the most upstream section of the Oder river, align very well (Figure **??**). Also, a very good agreement of the WSS variations with the lidar WSS can be seen at the Vistula River between chainage 350 km and 450 m.

The results of the reach-scale IRIS WSS are comparable to this study. This is probably also due to the fact that ICESat-2 altimeter measurements are also used as input data in this study. Only at the Oder River (33 mm/km vs. 6 mm/km) and at the Dunajec River (386 mm/km vs. 69 mm/km) the IRIS data show a significantly lower accuracy. Similar to the DEM-based approaches, the high mean RMSE of 81 mm/km is strongly influenced by the Dunajec River.

The WSS derived in this study are in agreement with WSS of Polish rivers reported in literature. There is no high-resolution information about WSS for short sections of Polish rivers available. However, there are several studies with general information about

mean WSS for selected river sections. The WSS of the entire Vistula River (divided into 12 sections) are provided by Starkel (2001). Considering only the sections overlapping with this study, the WSS by Starkel (2001) ranges from 360 mm/km in the upstream reach to 170 mm/km in the downstream reach. These values agree well with the WSS estimated in our study (cf. Figure **??**a). Although in some cases the WSS from this study exceeds the WSS by Starkel (2001), we derived the WSS for almost every kilometer of the river, whereas Starkel (2001) reported average WSS over long river sections. Habel (2010) conducted a WSS measurement campaign for the 60 km section of the Vistula between the Włocławek dam and the city of Toruń using a GNSS receiver mounted on a boat. The average slope for this section from two separate measurement campaigns is of 157 mm/km, which is almost identical to the mean WSS for the same section from this study (156 mm/km).

The WSS derived in this study shows high accuracy not only for the lowland rivers, but also for those located in mountainous areas. The WSS of the studied sections of the Dunajec River in the literature ranges from 580 mm/km to 3,350 mm/km (Pasternak, 1968), which agrees with the WSS from this study (cf. Figure **??**d). Although the WSE determination from satellite altimetry is challenging in steep-sided valleys (Jiang et al., 2020b), the difference between our results (2,930 mm/km) and a study by Nyka (2006) (3,200 mm/km) is relatively low for the Dunajec River Gorge.

In addition to the comparison with *in situ* and other WSS dataset, an internal cross-validation is performed comparing the WSS between two altimeter measurements with the WSS from this study. The resulting RMSD for the 11 Polish rivers varies between 16 mm/km and 300 mm/km, showing lower RMSD for the larger rivers and higher RMSD for the smaller mountain rivers. The cross-validation is a valuable tool to assess the WSS variation along the rivers because of the large amount of used altimeter measurements located at different river chainages. This method also allows us to assess the quality for river sections where no *in situ* data is available.

The WSS derived from satellite altimetry can also be useful for geomorphic and hydrologic applications. The accurate, high resolution WSS can significantly correct the altimetry-based WSE time series at virtual stations (Halicki et al., 2023; Scherer et al., 2022a). In this study, the RMSE of WSE time series is reduced by up to 42% for two virtual stations located at the San River and the Dunajec River. However, when WSE time series are affected by other errors such as the off-nadir effect, the WSS correction may be ineffective.

7 Conclusion and Outlook

In this study, we present an innovative approach to estimate high-resolution WSS of rivers based on multi-mission altimetry. We study 11 Polish rivers located in both lowland and mountainous areas. To maximize the spatial coverage of the altimetry measurements, we combine WSE from 11 satellites. The used missions are CryoSat-2, Envisat, ERS-1, ICESat-1/-2, Jason-2/-3, Saral, Sentinel-3A/-3B, and Sentinel-6A. The altimetry measurements cover the period from 1994 to 2022. In our approach, we first divide the rivers into river sections that are not interrupted by dams, waterfalls, or reservoirs. Then, we use a weighted least-squares adjustment with an additional Laplace condition and an *a priori* gradient condition to estimate the WSE at each river kilometer from which we derive the WSS.

The results of this study, are the most accurate WSS for Polish rivers from remote sensing data. The RMSE values for 11 investigated Polish rivers vary between 3 mm/km and 80 mm/km. It outperforms other WSS data especially in mountain rivers. The results of this study are compared with other global WSS datasets which are, however, limited in both quality and quantity. Existing global databases based on DEM models do not provide sufficient accuracy. Using WSS data from Ruetenik (2022) results in RMSE

values varying between 20 mm/km and 232 mm/km with an average of 65 mm/km. Using WSS data from Cohen et al. (2018) results in RMSE values varying between 294 mm/km and 2,742 mm/km (average: 732 mm/km). Using WSS from SWORD (Altenau et al., 2021a), the RMSE values vary between 29 mm/km and 273 mm/km (average: 86 mm/km). The comparison of using WSS data from the IRIS database (Scherer et al., 2022b) results in RMSE values between 5 mm/km and 386 mm/km (Average: 81 mm/km). Finally, the WSS from this study are compared with lidar data, resulting in RMSE values between 16 mm/km and 185 mm/km (Average: 84 mm/km) This study shows that the accuracy of WSS from satellite altimetry is high compared to WSS from the other sources shown. The advantage of accurate WSS of rivers is that the WSE time series at VS from satellite altimetry can be improved by correcting the ground track shift bias of the altimeter missions. For two examples at the San River and the Dunajec River, the RMSE of the WSE time series decreases by 42% and 41% respectively.

The SWOT mission, launched in December 2022, will also provide global WSS using state-of-the-art "radar interferometry", to monitor surface waters with unprecedented resolution. The scientific requirements of SWOT aim for a WSS accuracy of 17 mm/km (Biancamaria et al., 2016). The multi-mission satellite altimetry approach presented in this study shows an accuracy within the SWOT requirements for most of the rivers studied. Only the mountain rivers, i.e. San and Dunajec, have significantly lower accuracies. Since the WSS estimation approach can be applied globally, it can serve as validation data for the upcoming SWOT observations.

Appendix A WSS of the Pilica, San, Narew, Bug, Poprad, Noteć, and Wisłoka

Open Research

The results of this study are available at Zenodo via https://doi.org/10.5281/zenodo.7709474. The version 1.1 of the SWOT River Database (SWORD) is available at Zenodo via `https://doi.org/10.5281/zenodo.4917236` (Altenau et al., 2021a). The altimetry data are taken from the internal Multi-Version Altimetry (MVA) data holding of the Open Altimeter Database (OpenADB, `https://openadb.dgfi.tum.de` (Schwatke et al., 2023, in Review)) developed by the Deutsches Geodätisches Forschungsinstitut der Technischen Universität München (DGFI-TUM). Considering the validation datasets: (1) the lidar data are provided by the Polish Head Office of Geodesy and Cartography (Główny Urząd Geodezji i Kartografii) via `geoportal.gov.pl` (Kurczyński, 2015), (2) the reach-scale "ICESat-2 River Surface Slope" are available at Zenodo via `https://doi.org/10.5281/zenodo.7098114` (Scherer et al., 2022b) (3), the Global River Slopes (version 2.0) are available at `https://sdml.ua.edu/datasets-2/` (Cohen et al., 2018), and (4) the RiverProfileApp is available at `https://riverprofileapp.github.io/` (Ruetenik, 2022).

Acknowledgments

Michał Halicki acknowledges the financial support provided by the research project No. 2020/38/E/ST10/00295 within the Sonata BIS programme of the National Science Centre, Poland. Daniel Scherer acknowledges the financial support provided the Deutsche Forschungsgemeinschaft (DFG, German Research Foundation) - Project number 324641997, Grant DE 2174/10-2. We thank the Institute for Meteorology and Water Management – State Research Institute (IMGW-PIB) for providing the *in situ* data. We are also grateful to Tomasz Kolerski and Kacper Jancewicz for discussions on methodology. Open access funding enabled and organized by Projekt DEAL.

References

Abdalla, S., Abdeh Kolahchi, A., Ablain, M., Adusumilli, S., Aich Bhowmick, S., Alou-Font, E., ... Zlotnicki, V. (2021). Altimetry for the future: Building on 25 years of progress. *Advances in Space Research*, *68*(2), 319-363. doi: 10.1016/j.asr.2021.01.022

Allen, G. H., & Pavelsky, T. (2018). Global extent of rivers and streams. *Science*, *361*(6402), 585–588. doi: 10.1126/science.aat0636

Altenau, E. H., Pavelsky, T. M., Durand, M. T., Yang, X., d. M. Frasson, R. P., & Bendezu, L. (2021a, November). *Swot river database (sword).* Zenodo. doi: 10.5281/zenodo.5643392

Altenau, E. H., Pavelsky, T. M., Durand, M. T., Yang, X., Frasson, R. P. d. M., & Bendezu, L. (2021b). The Surface Water and Ocean Topography (SWOT) Mission River Database (SWORD): A Global River Network for Satellite Data Products. *Water Resources Research*, *57*(7). doi: 10.1029/2021WR030054

Altenau, E. H., Pavelsky, T. M., Moller, D., Lion, C., Pitcher, L. H., Allen, G. H., ... Smith, L. C. (2017, 16). AirSWOT measurements of river water surface elevation and slope: Tanana river, AK. *Geophysical Research Letters*, *44*(1), 181-189. doi: 10.1002/2016GL071577

Altenau, E. H., Pavelsky, T. M., Moller, D., Pitcher, L. H., Bates, P. D., Durand, M. T., & Smith, L. C. (2019). Temporal variations in river water surface elevation and slope captured by AirSWOT. *Remote Sensing of Environment*, *224*, 304-316. doi: 10.1016/j.rse.2019.02.002

Andrzejewski, L., & Starkel, L. (2018). Ewolucja systemów dolinnych i zmiany obiegu wody do od ustąpienia ostatniego zlodowacenia (Evolution of valley systems and changes in the water cycle since the end of the last glaciation). In P. Jokiel, W. Marszlewski, & J. Pociask-Karteczka (Eds.), *Hydrologia Polski (Hydrology of Poland)* (p. 111-116). Warsaw, Poland: PWN.

Bandini, F., Sunding, T. P., Linde, J., Smith, O., Jensen, I. K., Köppl, C. J., ... Bauer-Gottwein, P. (2020). Unmanned aerial system (UAS) observations of water surface elevation in a small stream: Comparison of radar altimetry, LIDAR and photogrammetry techniques. *Remote Sensing of Environment*, *237*, 111487. doi: 10.1016/j.rse.2019.111487

Biancamaria, S., Lettenmaier, D. P., & Pavelsky, T. M. (2016). The SWOT mission and its capabilities for land hydrology. *Surveys in Geophysics*, *37*(2), 307-337. doi: 10.1007/s10712-015-9346-y

Bielak, R., Borek, D., Głowacka-Smolis, K., Gustyn, J., Kozera, A., Kozłowska, J., ... Żelechowski, M. (2021). *Rocznik Statystyczny Rzeczypospolitej Polskiej (Statistical Yearbook of the Republic of Poland)* (Tech. Rep.). Warsaw, Poland: Główny Urząd Statystyczny (Statistics Poland).

Birkett, C. M. (2002). Surface water dynamics in the amazon basin: Application of satellite radar altimetry. *Journal of Geophysical Research*, *107*(D20), 8059. doi: 10.1029/{2001JD000609}

Bjerklie, D. M., Lawrence Dingman, S., Vorosmarty, C. J., Bolster, C. H., & Congalton, R. G. (2003). Evaluating the potential for measuring river discharge from space. *Journal of Hydrology*, *278*(1-4), 17-38. doi: 10.1016/S0022-1694(03)00129-X

Boergens, E., Dettmering, D., Schwatke, C., & Seitz, F. (2016). Treating the Hooking Effect in Satellite Altimetry Data: A Case Study along the Mekong River and Its Tributaries. *Remote Sensing*, *8*(2), 91. doi: 10.3390/rs8020091

Bogning, S., Frappart, F., Blarel, F., Niño, F., Mahé, G., Bricquet, J.-P., ... Braun, J.-J. (2018). Monitoring Water Levels and Discharges Using Radar Altimetry in an Ungauged River Basin: The Case of the Ogooué. *Remote Sensing*, *10*(3), 350. doi: 10.3390/rs10020350

Bosch, W., Dettmering, D., & Schwatke, C. (2014). Multi-Mission Cross-Calibration of Satellite Altimeters: Constructing a Long-Term Data Record for Global and

Regional Sea Level Change Studies. *Remote Sensing*, *6*(3), 2255–2281. doi: 10.3390/rs6032255

Calmant, S., & Seyler, F. (2006). Continental surface waters from satellite altimetry. *Comptes Rendus Geoscience*, *338*(14-15), 1113-1122. doi: 10.1016/j.crte.2006.05.012

Cohen, S., Wan, T., Islam, M. T., & Syvitski, J. (2018). Global river slope: A new geospatial dataset and global-scale analysis. *Journal of Hydrology*, *563*, 1057-1067. doi: 10.1016/j.jhydrol.2018.06.066

Deidda, C., De Michele, C., Arslan, A., Pecora, S., & Taburet, N. (2021). Accuracy of Copernicus Altimeter Water Level Data in Italian Rivers Accounting for Narrow River Sections. *Remote Sensing*, *13*(21), 4456. doi: 10.3390/rs13214456

Dębski, K. (1970). *Hydrologia (Hydrology)*. Warsaw, Poland: Arkady.

Durand, M., Neal, J., Rodríguez, E., Andreadis, K. M., Smith, L. C., & Yoon, Y. (2014). Estimating reach-averaged discharge for the River Severn from measurements of river water surface elevation and slope. *Journal of Hydrology*, *511*, 92-104. doi: 10.1016/j.jhydrol.2013.12.050

Dynowska, I. (1997). *Reżim odpływu rzecznego (River runoff regime)* [MAP]. Warsaw, Poland: Wydawnictwo Naukowe PWN.

Gleason, C. J., & Durand, M. T. (2020). Remote sensing of river discharge: A review and a framing for the discipline. *Remote Sensing*, *12*(7), 1–28. doi: 10.3390/rs12071107

Habel, M. (2010). Zróżnicowanie podłużnego spadku zwierciadła wody w korycie Wisły poniżej Zbiornika Włocławskiego (Diversity of longitudinal slopes of water surface on the Vistula Channel below Wloclawek reservoir). *Studia i Prace z Geografii i Geologii*, *19*, 36-46.

Halicki, M., & Niedzielski, T. (2022). The accuracy of the Sentinel-3A altimetry over Polish rivers. *Journal of Hydrology*, *606*, 127355. doi: 10.1016/j.jhydrol.2021.127355

Halicki, M., Schwatke, C., & Niedzielski, T. (2023). The impact of the satellite ground track shift on the accuracy of altimetric measurements on rivers: a case study of the Sentinel-3 altimetry on the Odra/Oder River. *Journal of Hydrology*, *617*, 128761. doi: 10.1016/j.jhydrol.2022.128761

Hall, A. C., Schumann, G. J.-P., Bamber, J. L., Bates, P. D., & Trigg, M. A. (2012). Geodetic corrections to Amazon River water level gauges using ICESat altimetry. *Water Resources Research*, *48*(6). doi: 10.1029/2011WR010895

Hannah, D. M., Demuth, S., van Lanen, H. A. J., Looser, U., Prudhomme, C., Rees, G., ... Tallaksen, L. M. (2011). Large-scale river flow archives: importance, current status and future needs. *Hydrological Processes*, *25*(7), 1191-1200. doi: 10.1002/hyp.7794

Hwang, C., Guo, J., Deng, X., Hsu, H.-Y., & Liu, Y. (2006). Coastal gravity anomalies from retracked geosat/GM altimetry: Improvement, limitation and the role of airborne gravity data. *Journal of Geodesy*, *80*(4), 204–216. doi: 10.1007/s00190-006-0052-x

IMGW-PIB. (2013). *Raport końcowy z wykonania map zagrożenia powodziowego i map ryzyka powodziowego (Final report on the preparation of flood hazard maps and flood risk maps)* (Tech. Rep.). IMGW-PIB. Retrieved 2022-09-01, from `https://www.kzgw.gov.pl/files/mzp-mrp/zal1.pdf`

Jiang, L., Bandini, F., Smith, O., Klint Jensen, I., & Bauer-Gottwein, P. (2020a). The Value of Distributed High-Resolution UAV-Borne Observations of Water Surface Elevation for River Management and Hydrodynamic Modeling. *Remote Sensing*, *12*(7), 1171. doi: 10.3390/rs12071171

Jiang, L., Nielsen, K., Dinardo, S., Andersen, O. B., & Bauer-Gottwein, P. (2020b). Evaluation of Sentinel-3 SRAL SAR altimetry over Chinese rivers. *Remote Sensing of Environment*, *237*, 111546. doi: 10.1016/j.rse.2019.111546

Kittel, C. M. M., Jiang, L., Tøttrup, C., & Bauer-Gottwein, P. (2021). Sentinel-3 radar altimetry for river monitoring – a catchment-scale evaluation of satellite water surface elevation from Sentinel-3A and Sentinel-3B. *Hydrology and Earth System Sciences*, *25*(1), 333-357. doi: 10.5194/hess-25-333-2021

Kurczyński, Z. (2015). Lotnicze skanowanie laserowe – podstawy teoretyczne (Aerial laser scanning - theoretical foundations). In P. Wężyk (Ed.), *Podręcznik dla uczestników szkoleń z wykorzystania produktów LiDAR (Manual for participants of training on the use of LiDAR products)* (pp. 59–111). Warsaw, Poland. Retrieved from `http://www.gugik.gov.pl/__data/assets/pdf_file/0019/23752/PODRECZNIK_ISOK_wyd.2.pdf`

Lamine, B., Ferreira, V., Yang, Y., Ndehedehe, C., & He, X. (2021). Estimation of the niger river cross-section and discharge from remotely-sensed products. *Journal of Hydrology: Regional Studies*, *36*, 100862. doi: 10.1016/j.ejrh.2021.100862

LeFavour, G., & Alsdorf, D. (2005). Water slope and discharge in the Amazon River estimated using the shuttle radar topography mission digital elevation model. *Geophysical Research Letters*, *32*(17). doi: 10.1029/{2005GL023836}

Lehner, B., Verdin, K., & Jarvis, A. (2008). New Global Hydrography Derived From Spaceborne Elevation Data. *Eos, Transactions American Geophysical Union*, *89*(10), 93-94. doi: 10.1029/2008EO100001

Manning, R. (1891). On the ow of water in open channels and pipes. *Transactions of the Institution of Civil Engineers of Ireland*, *20*, 161-207.

Migoń, P. (2006). *Geomorfologia (Geomporhology)*. Warsaw, Poland: PWN.

Miętus, M., Biernacik, D., Chodubska, A., Marosz, M., Łaszyca, E., & Kitowski, M. (2022). *Wstępna analiza klimatyczna 2021 (Preliminary climate analysis 2021)* (Tech. Rep.). Retrieved 2022-12-08, from `https://www.imgw.pl/sites/default/files/2022-01/imgw\_0126-wstepna-analiza-klimatyczna-2021.pdf`

Niemeier, W. (2008). *Ausgleichungsrechnung: Statistische auswertemethoden (2.auflage)*. Walter de Gruyter.

Normandin, C., Frappart, F., Diepkilé, A. T., Marieu, V., Mougin, E., Blarel, F., ... Ba, A. (2018, 25). Evolution of the Performances of Radar Altimetry Missions from ERS-2 to Sentinel-3A over the Inner Niger Delta. *Remote Sensing*, *10*(6), 833-860. doi: 10.3390/rs10060833

Nyka, J. (2006). *Pieniny* (IX ed.). Latchorzew, Poland: Trawers.

O'Loughlin, F., Trigg, M. A., Schumann, G. J.-P., & Bates, P. D. (2013). Hydraulic characterization of the middle reach of the Congo River. *Water Resources Research*, *49*(8), 5059-5070. doi: 10.1002/wrcr.20398

Ozga-Zielińska, M., & Brzeziński, J. (1997). *Hydrologia stosowana (Applied hydrology)*. Warsaw, Poland: PWN.

Paris, A., Dias de Paiva, R., Santos da Silva, J., Medeiros Moreira, D., Calmant, S., Garambois, P.-A., ... Seyler, F. (2016). Stage-discharge rating curves based on satellite altimetry and modeled discharge in the Amazon basin. *Water Resources Research*, *52*(5), 3787-3814. doi: 10.1002/{2014WR016618}

Pasternak, K. (1968). Charakterystyka podłoża zlewni rzeki Dunajec (Characteristics of the substratum of the River Dunajec catchment basin). *Acta Hydrobiologica*, *10*(3), 299-317.

Paz, A. R., & Collischonn, W. (2007). River reach length and slope estimates for large-scale hydrological models based on a relatively high-resolution digital elevation model. *Journal of Hydrology*, *343*(3-4), 127-139. doi: 10.1016/j.jhydrol.2007.06.006

Peel, M. C., Finlayson, B. L., & McMahon, T. A. (2007, 11). Updated world map of the Köppen-Geiger climate classification. *Hydrology and Earth System Sciences*, *11*(5), 1633-1644. doi: 10.5194/hess-11-1633-2007

Pitcher, L. H., Pavelsky, T. M., Smith, L. C., Moller, D. K., Altenau, E. H., Allen,

G. H., ... Bertram, M. (2019). AirSWOT InSAR Mapping of Surface Water Elevations and Hydraulic Gradients Across the Yukon Flats Basin, Alaska. *Water Resources Research*, *55*(2), 937-953. doi: 10.1029/{2018WR023274}

Pociask-Karteczka, J. (2018). Położenie hydrograficzne Polski na tle Europy (The hydrographic location of Poland against the background of Europe). In P. Jokiel, W. Marszlewski, & J. Pociask-Karteczka (Eds.), *Hydrologia Polski (Hydrology of Poland)* (p. 15-21). Warsaw, Poland: PWN.

Rantz, S. E. (1982). *Measurement and computation of streamflow* (Tech. Rep.). United States Geological Survey. doi: 10.3133/wsp2175

Rodríguez, E., Morris, C. S., & Belz, J. E. (2006). A global assessment of the SRTM performance. *Photogrammetric Engineering and Remote Sensing*, *72*(3), 249-260. doi: 10.14358/PERS.72.3.249

Ruetenik, G. A. (2022). Introducing RiverProfileApp, a web application for near-global, exploratory, longitudinal river profile analysis. *International Journal of Digital Earth*, *15*(1), 679-689. doi: 10.1080/17538947.2022.2055173

Santos da Silva, J., Calmant, S., Seyler, F., Rotunno Filho, O. C., Cochonneau, G., & Mansur, W. J. (2010). Water levels in the Amazon basin derived from the ERS 2 and ENVISAT radar altimetry missions. *Remote Sensing of Environment*, *114*(10), 2160-2181. doi: 10.1016/j.rse.2010.04.020

Scherer, D., Schwatke, C., Dettmering, D., & Seitz, F. (2020). Long-Term Discharge Estimation for the Lower Mississippi River Using Satellite Altimetry and Remote Sensing Images. *Remote Sensing*, *12*(17), 2693. doi: 10.3390/rs12172693

Scherer, D., Schwatke, C., Dettmering, D., & Seitz, F. (2022a). ICESat-2 Based River Surface Slope and Its Impact on Water Level Time Series From Satellite Altimetry. *Water Resources Research*, *58*(11), e2022WR032842. doi: 10.1029/2022WR032842

Scherer, D., Schwatke, C., Dettmering, D., & Seitz, F. (2022b). *IRIS: ICESat-2 River Surface Slope.* Zenodo. doi: 10.5281/zenodo.7098114

Scherer, D., Schwatke, C., Dettmering, D., & Seitz, F. (In Review). *ICESat-2 River Surface Slope (IRIS): A Global Reach-Scale Water Surface Slope Dataset.* (In Review)

Schumann, G., Matgen, P., Cutler, M., Black, A., Hoffmann, L., & Pfister, L. (2008). Comparison of remotely sensed water stages from LiDAR, topographic contours and SRTM. *ISPRS Journal of Photogrammetry and Remote Sensing*, *63*(3), 283-296. doi: 10.1016/j.isprsjprs.2007.09.004

Schwatke, C., Dettmering, D., Börgens, E., & Bosch, W. (2015a). Potential of saral/altika for inland water applications. *Marine Geodesy*, *38*(sup1), 626-643. doi: 10.1080/01490419.2015.1008710

Schwatke, C., Dettmering, D., Bosch, W., & Seitz, F. (2015b). DAHITI – an innovative approach for estimating water level time series over inland waters using multi-mission satellite altimetry. *Hydrology and Earth System Sciences*, *19*(10), 4345–4364. doi: 10.5194/hess-19-4345-2015

Schwatke, C., Dettmering, D., Passaro, M., Hart-Davis, M., Scherer, D., Müller, F. L., ... Seitz, F. (In Review). OpenADB: DGFI-TUM's Open Altimeter Database. *Geoscience Data Journal*, *xxx*, xxx-xxx. doi: 10.1016/j.rse.2015.05.025

Schwatke, C., Halicki, M., & Scherer, D. (2023b). *High-Resolution Water Surface Slopes from Multi-Mission Satellite Altimetry.* Zenodo. doi: 10.5281/zenodo.7709474

Smola, A. J., & Schölkopf, B. (2004). A tutorial on support vector regression. *Statistics and Computing*, *14*(3), 199-222. doi: 10.1023/B:STCO.0000035301.49549.88

Starkel, L. (2001). Budowa geologiczna i rzeźba dorzecza Wisły (Geological structure and relief of the Vistula river basin). In *Historia doliny Wisły od ostat-*

niego zlodowacenia do dziś (Evolution of the Vistula River valley since the last glaciation till present) (p. 12-15). Warsaw, Poland: PAN.

Tarpanelli, A., Barbetta, S., Brocca, L., & Moramarco, T. (2013, aug 22). River Discharge Estimation by Using Altimetry Data and Simplified Flood Routing Modeling. *Remote Sensing*, *5*(9), 4145-4162. doi: 10.3390/rs5094145

Tourian, M., Schwatke, C., & Sneeuw, N. (2017). River discharge estimation at daily resolution from satellite altimetry over an entire river basin. *Journal of Hydrology*, *546*, 230-247. doi: 10.1016/j.jhydrol.2017.01.009

Tourian, M., Tarpanelli, A., Elmi, O., Qin, T., Brocca, L., Moramarco, T., & Sneeuw, N. (2016). Spatiotemporal densification of river water level time series by multimission satellite altimetry. *Water Resources Research*, *52*(2), 1140-1159. doi: 10.1002/2015WR017654

Tuozzolo, S., Lind, G., Overstreet, B., Mangano, J., Fonstad, M., Hagemann, M., ... Durand, M. (2019, feb 16). Estimating River Discharge With Swath Altimetry: A Proof of Concept Using AirSWOT Observations. *Geophysical Research Letters*, *46*(3), 1459-1466. doi: 10.1029/2018GL080771

Villadsen, H., Andersen, O. B., Stenseng, L., Nielsen, K., & Knudsen, P. (2015). CryoSat-2 altimetry for river level monitoring – Evaluation in the Ganges-Brahmaputra River basin. *Remote Sensing of Environment*, *168*, 80-89. doi: 10.1016/j.rse.2015.05.025

Vorosmarty, C., Askew, A., Grabs, W., Barry, R. G., Birkett, C., Döll, P., ... Webster, F. (2001). Global water data: A newly endangered species. *Eos, Transactions American Geophysical Union*, *82*(5), 54-54. doi: 10.1029/01EO00031

Wrzesiński, D. (2018). Reżimy rzek Polski (Regimes of Polish rivers). In P. Jokiel, W. Marszlewski, & J. Pociask-Karteczka (Eds.), *Hydrologia Polski (Hydrology of Poland)* (p. 215-221). Warsaw, Poland: PWN.

Yamazaki, D., Ikeshima, D., Sosa, J., Bates, P. D., Allen, G. H., & Pavelsky, T. M. (2019). MERIT Hydro: A High-Resolution Global Hydrography Map Based on Latest Topography Dataset. *Water Resources Research*, *55*(6), 5053–5073. doi: 10.1029/2019WR024873

Figure 1.

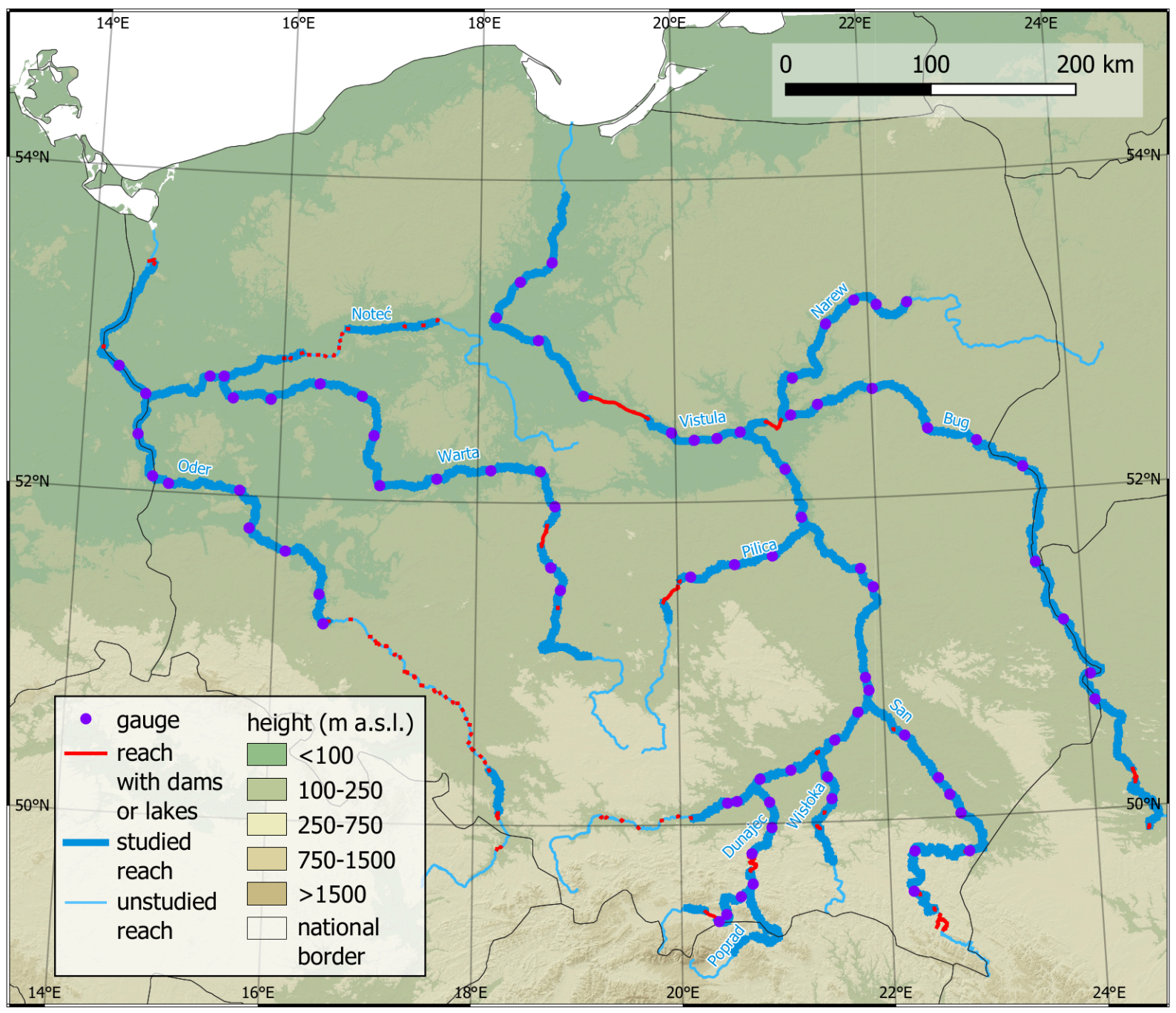
14°E
16°E
18°E
20°E
22°E
24°E
54°N
52°N
50°N
0
100
200 km
Noteć
Narew
Vistula
Bug
Oder
Warta
Pilica
San
Wisloka
Dunajec
Poprad
gauge
reach with dams or lakes
studied reach
unstudied reach
height (m a.s.l.)
<100
100-250
250-750
750-1500
>1500
national border

Figure 2.

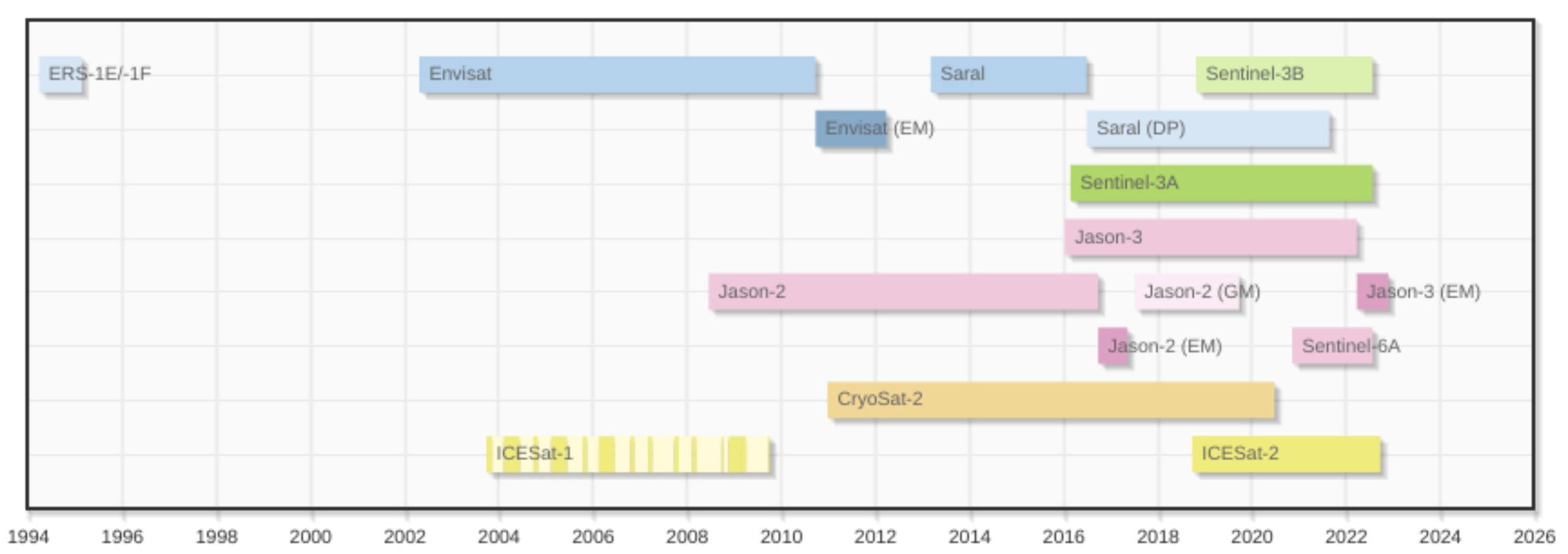
ERS-1E/-1F
Envisat
Saral
Sentinel-3B
Envisat (EM)
Saral (DP)
Sentinel-3A
Jason-3
Jason-2
Jason-2 (GM)
Jason-3 (EM)
Jason-2 (EM)
Sentinel-6A
CryoSat-2
ICESat-1
ICESat-2
1994
1996
1998
2000
2002
2004
2006
2008
2010
2012
2014
2016
2018
2020
2022
2024
2026

Figure 3.

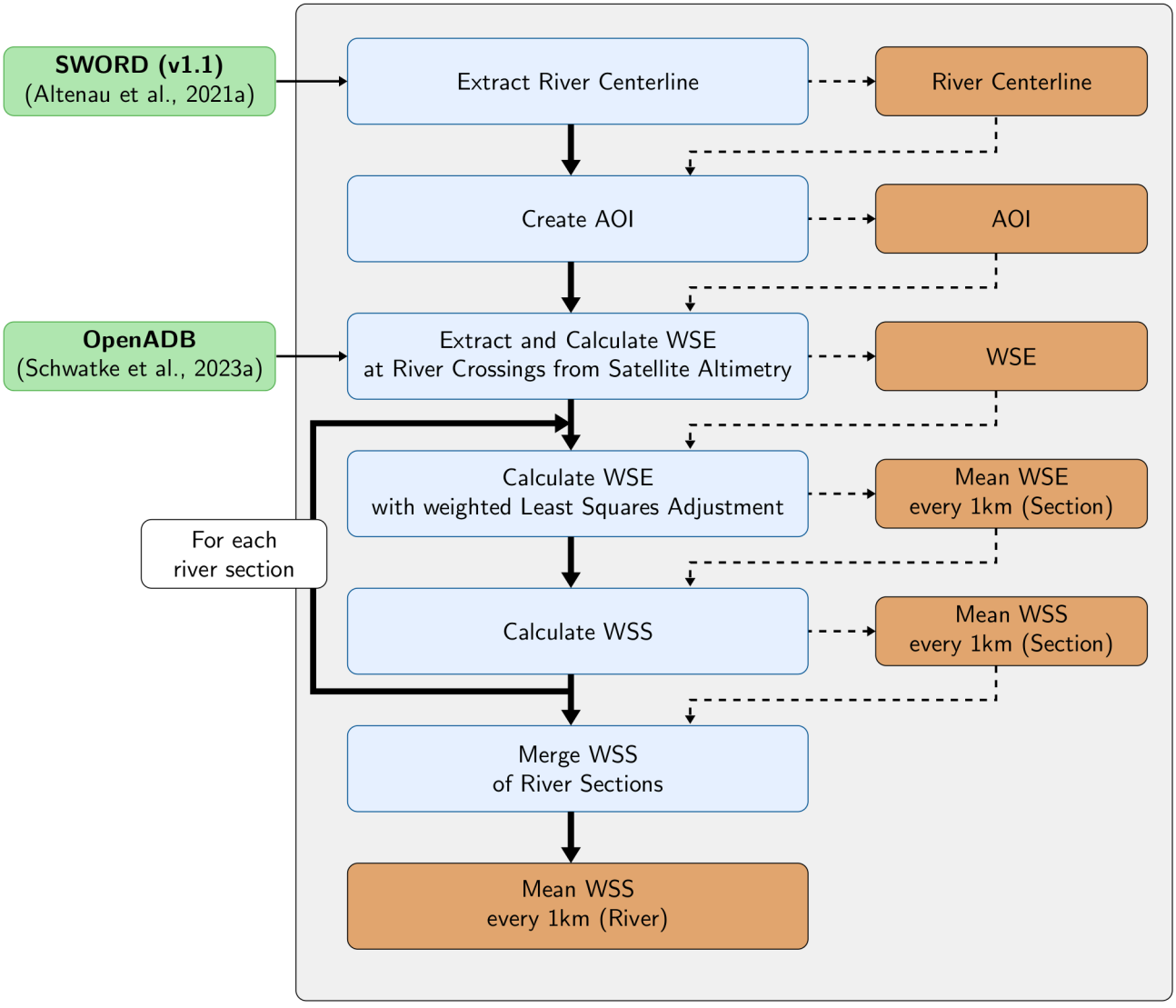
SWORD (v1.1)
(Altenau et al., 2021a)
OpenADB
(Schwatke et al., 2023a)
Extract River Centerline
River Centerline
Create AOI
AOI
Extract and Calculate WSE
at River Crossings from Satellite Altimetry
WSE
Calculate WSE
with weighted Least Squares Adjustment
Mean WSE
every 1km (Section)
For each
river section
Calculate WSS
Mean WSS
every 1km (Section)
Merge WSS
of River Sections
Mean WSS
every 1km (River)

Figure 4.

Altimeter Missions

- SARAL (DP)
- Envisat (EM)
- Envisat, SARAL
- Sentinel-3A
- Sentinel-3B
- Cryosat-2
- ICESat-1/-2
- ERS-1E/-1F
- Jason-2 (GM)
- Jason-2/-3 (EM)
- Jason-2/-3, Sentinel-6A

Centerline (1 km bins)

AOI

Świecie

Chełmno

Grudziądz

0 1 km

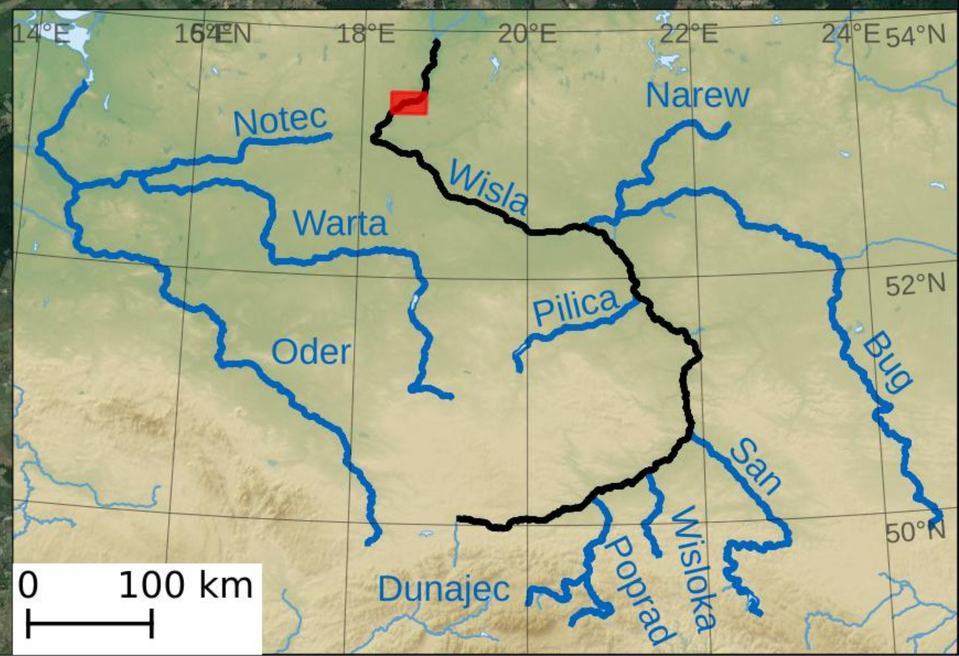

Figure 5.

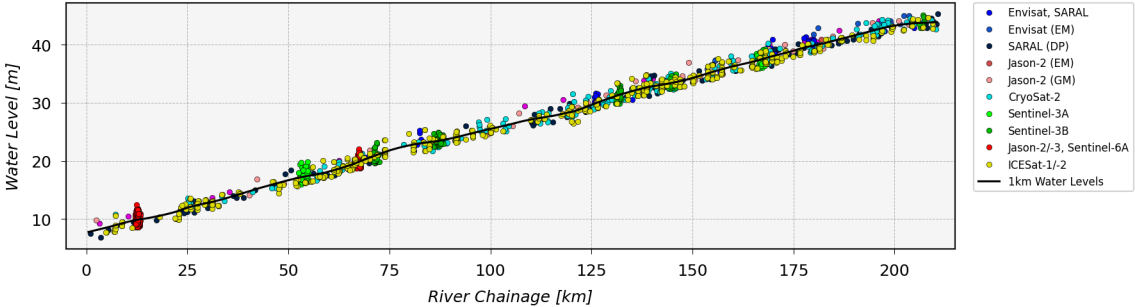
Water Level [m]
River Chainage [km]
10
20
30
40
0
25
50
75
100
125
150
175
200
Envisat, SARAL
Envisat (EM)
SARAL (DP)
Jason-2 (EM)
Jason-2 (GM)
CryoSat-2
Sentinel-3A
Sentinel-3B
Jason-2/-3, Sentinel-6A
ICESat-1/-2
1km Water Levels

Figure 6.

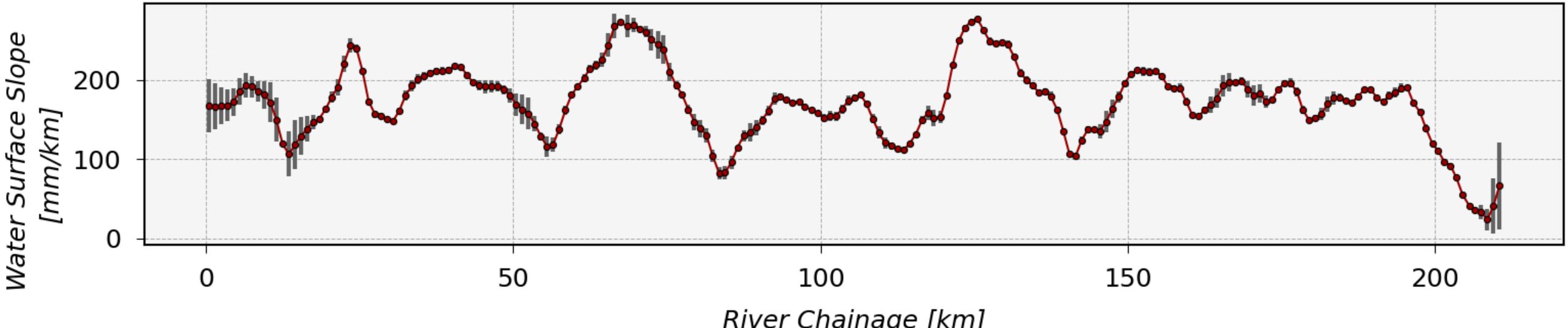
Water Surface Slope
[mm/km]
200
100
0
0
50
100
150
200
River Chainage [km]

Figure 7.

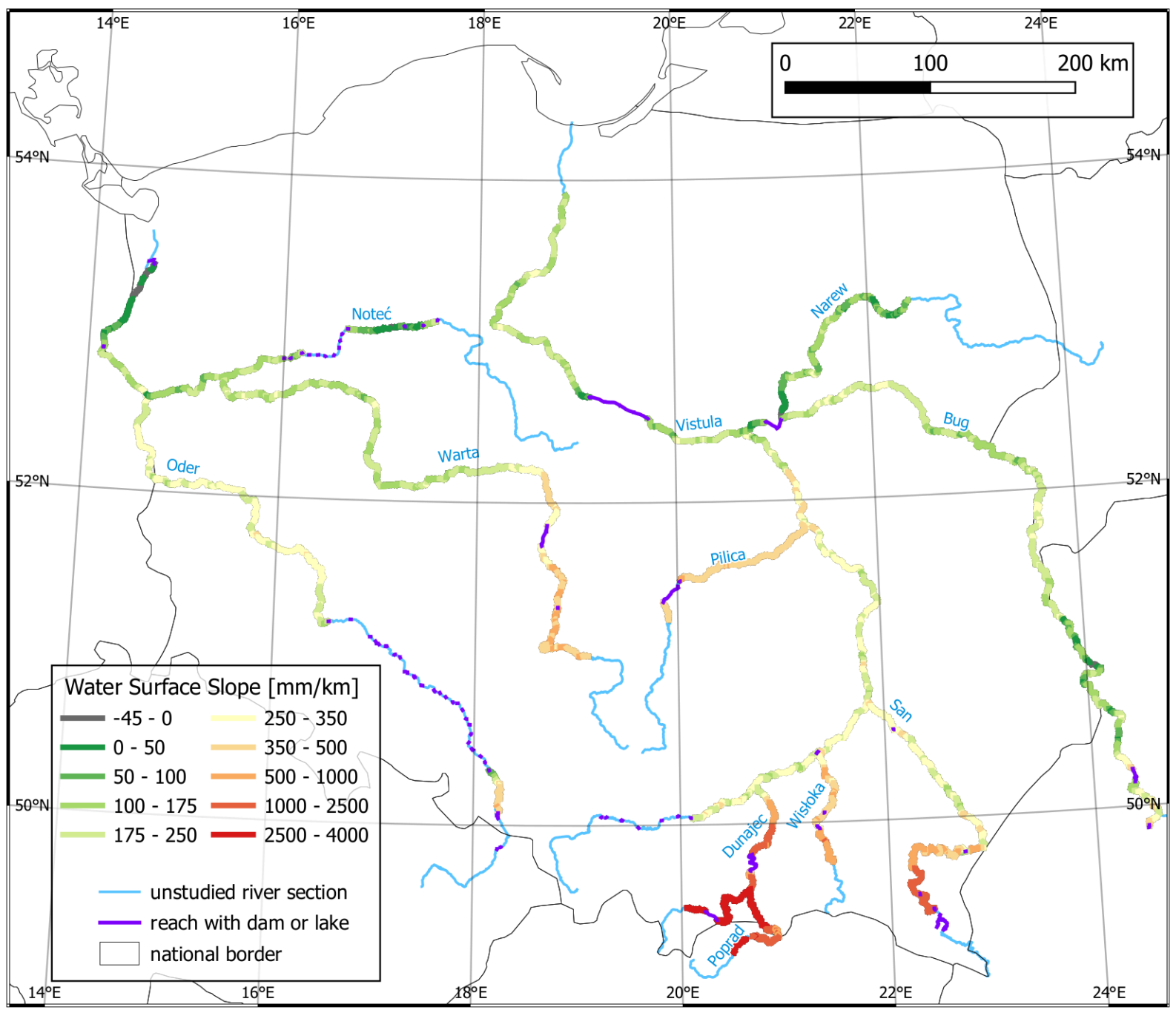
14°E
16°E
18°E
20°E
22°E
24°E
54°N
52°N
50°N
0
100
200 km
Noteć
Narew
Vistula
Bug
Oder
Warta
Pilica
San
Dunajec
Wisloka
Poprad
Water Surface Slope [mm/km]
-45 - 0
0 - 50
50 - 100
100 - 175
175 - 250
250 - 350
350 - 500
500 - 1000
1000 - 2500
2500 - 4000
unstudied river section
reach with dam or lake
national border

Figure 8.

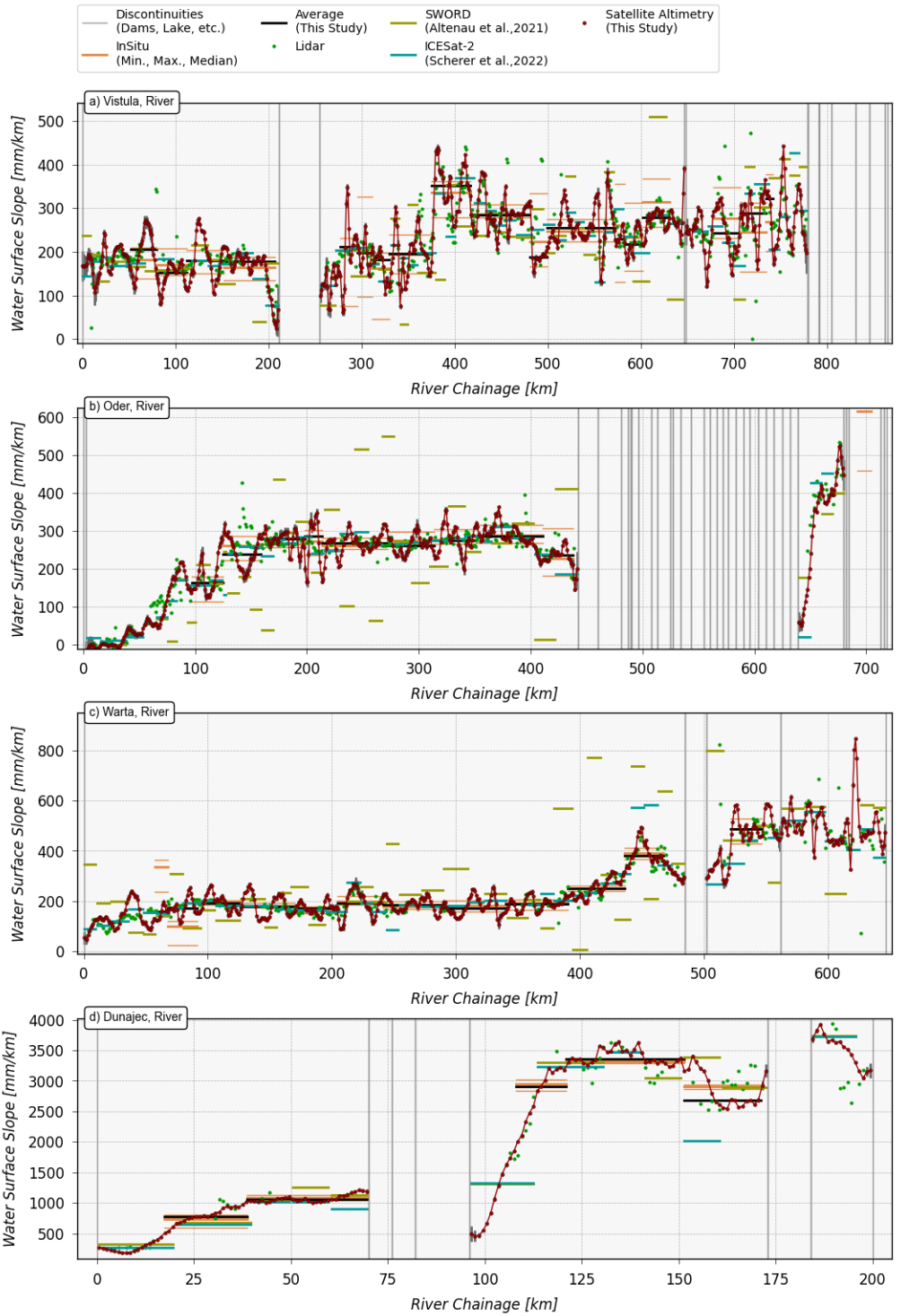
Discontinuities (Dams, Lake, etc.)
InSitu (Min., Max., Median)
Average (This Study)
Lidar
SWORD (Altenau et al.,2021)
ICESat-2 (Scherer et al.,2022)
Satellite Altimetry (This Study)
a) Vistula, River
b) Oder, River
c) Warta, River
d) Dunajec, River
Water Surface Slope [mm/km]
River Chainage [km]

Figure 9.


DAHITI (orignal) / RMSE: 0.36 m
DAHITI (corrected) / RMSE: 0.21 m
Water Level [m]
194
193
192
191
190
189
2020
2021
2022
2023
Distance to Ref. Location
Distance [km]
2
0
Slope corrected (553 [mm/km])
Slope not corrected
In-Situ Diff. [m]
1
0

Figure 10.

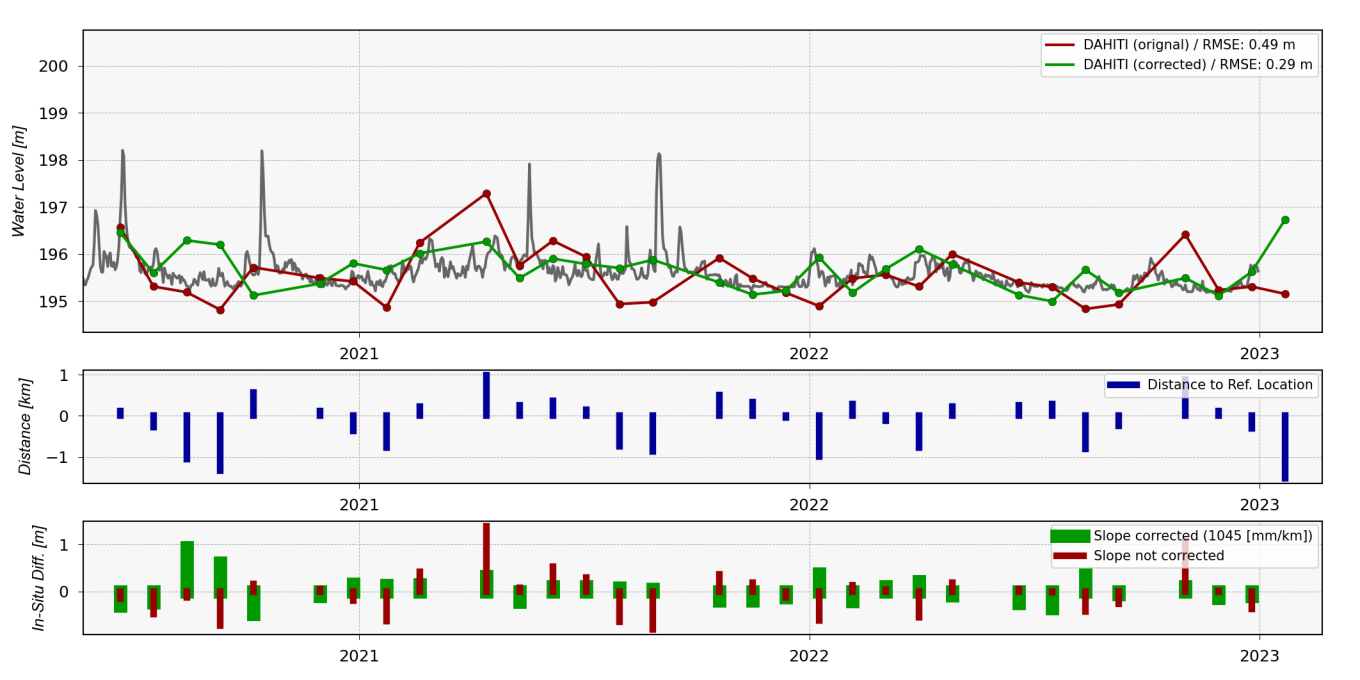
DAHITI (orignal) / RMSE: 0.49 m
DAHITI (corrected) / RMSE: 0.29 m
Water Level [m]
200
199
198
197
196
195
2021
2022
2023
Distance to Ref. Location
Distance [km]
1
0
−1
2021
2022
2023
Slope corrected (1045 [mm/km])
Slope not corrected
In-Situ Diff. [m]
1
0
2021
2022
2023

Figure A1.

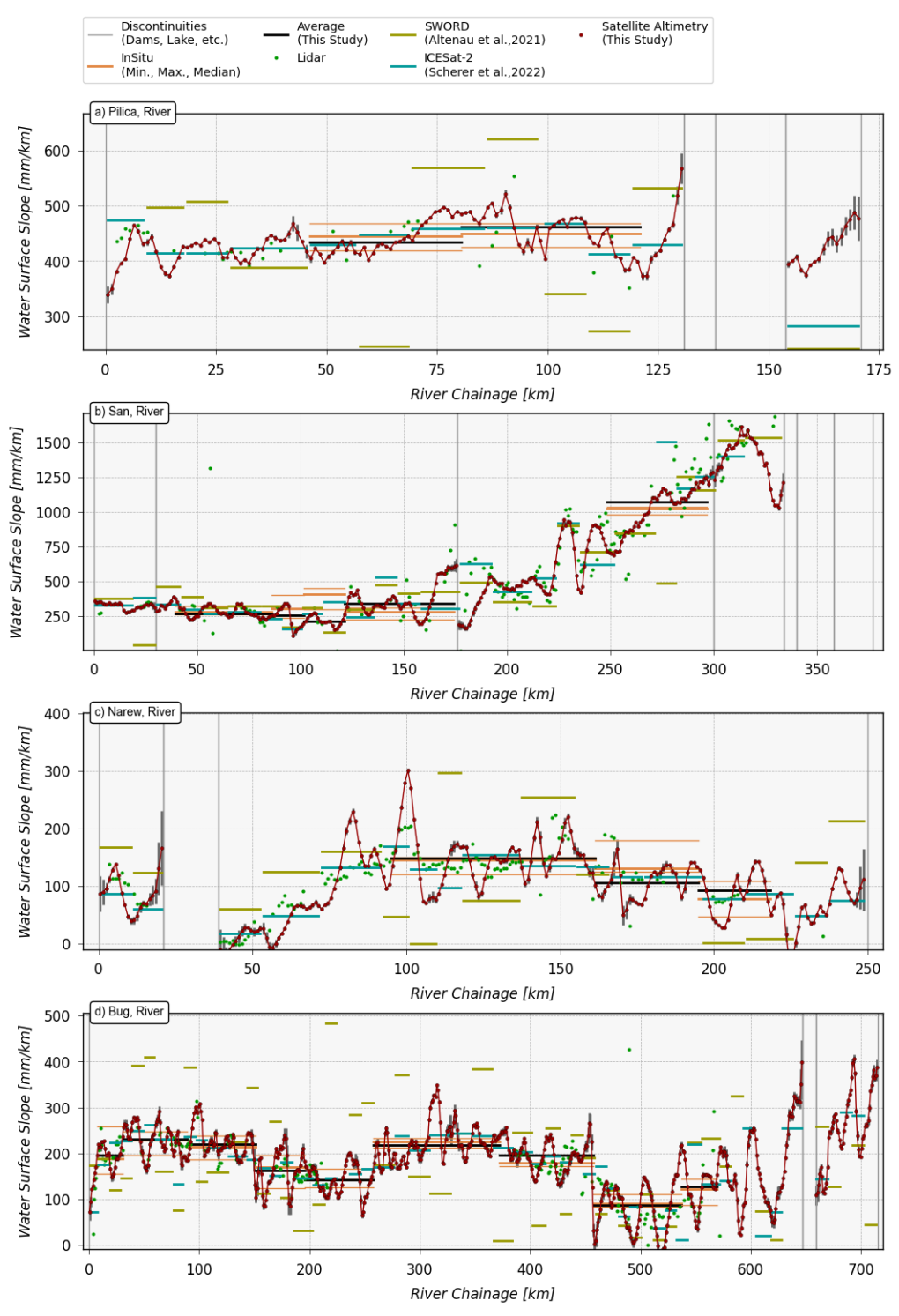
Discontinuities (Dams, Lake, etc.)
InSitu (Min., Max., Median)
Average (This Study)
Lidar
SWORD (Altenau et al.,2021)
ICESat-2 (Scherer et al.,2022)
Satellite Altimetry (This Study)
a) Pilica, River
b) San, River
c) Narew, River
d) Bug, River
Water Surface Slope [mm/km]
River Chainage [km]

Figure A2.

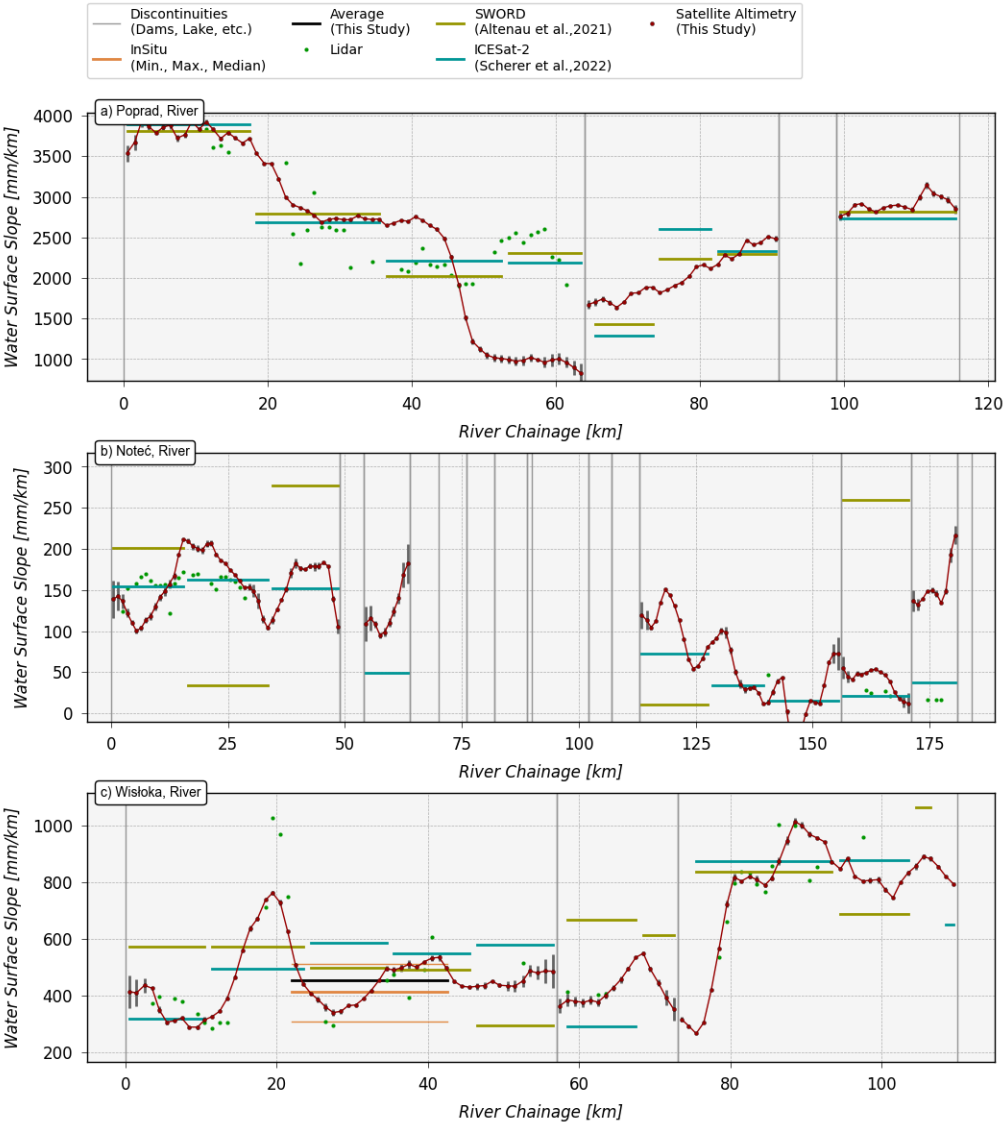
Discontinuities (Dams, Lake, etc.)
InSitu (Min., Max., Median)
Average (This Study)
Lidar
SWORD (Altenau et al.,2021)
ICESat-2 (Scherer et al.,2022)
Satellite Altimetry (This Study)
a) Poprad, River
b) Noteć, River
c) Wisłoka, River
Water Surface Slope [mm/km]
River Chainage [km]